



**NTNU – Trondheim**  
Norwegian University of  
Science and Technology

# Properties of thermal sprayed coatings for internal use in pipes and bends

**André Sunde**

Subsea Technology

Submission date: June 2015

Supervisor: Olav Egeland, IPK

Co-supervisor: Roy Johnsen, IPM

Norwegian University of Science and Technology  
Department of Production and Quality Engineering



André Sunde, NTNU

# Properties of thermal sprayed coatings for internal use in pipes and bends

Master thesis

Trondheim, May 2015

Supervisor: Roy Johnsen

Norwegian university of science and technology

Faculty of engineering science and technology

Department of engineering design and materials



**NTNU – Trondheim**  
Norwegian University of  
Science and Technology



## Abstract

NTNU/SINTEF are participating in a research project called “Smooth Surfaces”, financed by Norsk Forskningsråd, and with Brunvoll, Triplex, Omya Hustadmarmor and Aquamarine as industry partners in the project.

One of the activities in this project is named “internal corrosion- and wear protection of pipes by means of thermal spraying”.

The objective of this master thesis has been to document main properties for thermal sprayed coatings for internal use in pipes and bends. The main properties in question are; wear resistance, corrosion, hardness, ductility and porosity.

Different methods of thermal spray were evaluated based on specified requirements and High Velocity Oxy-Fuel (HVOF) was selected as the preferred method of applying the coating. As for the coating material itself, Amperit 560 was selected due to its references as a proven material for corrosion and erosion protection of equipment.

Hence, the scope of this master thesis has been to document the properties of the thermal sprayed Amperit 560 coating. The parameters used when thermally spraying the test samples simulates the spraying conditions present when spraying internal surfaces of pipes. Samples thermally sprayed with an angle of 45 and 90 degrees were supplied to compare the quality.

The main requirement of the coating is to provide erosion and corrosion resistance. These properties were documented using an electrochemical porosity test and an erosion test using a water slurry containing alumina. Tests to characterize the mechanical properties of the coating were done as well. These tests includes examination of microstructure and measuring of hardness, roughness and adhesion strength. The behaviour of the coating during bending of the surface and shock impacts is also included.

## Sammendrag

NTNU/SINTEF deltar i et forskningsprosjekt kalt "Glatte flater", finansiert av Norsk Forskningsråd, og med Brunvoll, Triplex, Omya Hustadmarmor og Aquamarine som industripartnere i prosjektet.

En av aktivitetene i dette prosjektet er "Innvendig korrosjons- og slitasjebeskyttelse av rør ved hjelp av termisk sprøyting".

Målet med denne masteroppgaven har vært å dokumentere de viktigste egenskapene til termisk sprøytete belegg for innvendig bruk i rør og bend. Egenskapene som skal dokumenteres er; slitasje, korrosjon, hardhet, duktilitet og porøsitet.

Ulike metoder for termisk sprøyting ble vurdert basert på spesifikke krav og High Velocity Oxy-Fuel (HVOF) ble valgt som den foretrukne metoden for påføring av belegg. For beleggmaterialiet ble Ampert 560 valgt, grunnet gode referanser for gode egenskaper for korrosjons- og erosjonsbeskyttelse av utstyr.

Ut fra nevnte mål har rammen til denne masteroppgaven vært å dokumentere egenskapene til det termisk sprøytete Ampert 560 belegget. Parameterne brukt for å termisk sprøyte prøvestykkene har blitt gjort under forhold som simulerer innvendige overflater i rør. Prøvestykker med sprøytevinkel på både 45 og 90 grader er testet for å sammenligne resultater og kvalitet på belegget.

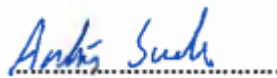
Hovedoppgaven til belegget er å beskytte mot erosjon og korrosjon. Disse egenskapene ble dokumentert ved hjelp av en elektrokjemisk porøsitetstest, og en erosjonstest ved bruk av en blanding av vann og aluminiumoksid. Tester brukt for å karakterisere de mekaniske egenskapene til belegget ble gjort i tillegg. Disse testene inkluderer undersøkelse av mikrostruktur og måling av hardhet, ruhet og adhesjonsstyrke. Beleggets oppførsel under bøyning og slag er også sett på.

## Preface

This thesis is made as a completion of a master degree at the Norwegian university of science and technology, faculty of engineering science and technology, department of engineering design and materials. The work of this thesis were performed during the spring semester in 2015.

Several persons have contributed with academically and practical support during the work of this master thesis. I would like to thank my supervisor Roy Johnsen for helpful feedback and suggestions during the work of the thesis. Furthermore, I would like to thank Cristian Torres and Shawn Wilson for help and guidance during the experiments. The assistance received from the personnel in the labs and workshops during setup and testing have been of great help and I would like to thank them as well.

Trondheim, June 2015

A handwritten signature in blue ink, reading "André Sunde", is positioned above a horizontal dotted line.

André Sunde

## Table of contents

1	Introduction .....	1
1.1	Background .....	1
1.2	Development of a new solution .....	2
1.3	The environment experienced in the pipes .....	3
1.4	Challenges regarding internal spraying of pipes .....	4
1.5	Purpose and composition of report .....	4
2	Thermal spraying.....	5
2.1	Methods of thermal spray .....	6
2.1.1	Combustion .....	7
2.1.2	Detonation.....	9
2.1.3	Electrical spray .....	10
2.1.4	Cold spray .....	12
2.2	Comparison of HVOF and cold spray method .....	13
2.3	Coatings .....	16
2.3.1	Wear resistance.....	16
2.3.2	Corrosion resistance.....	21
3	Testing.....	23
3.1	Samples for testing .....	23
3.2	Microstructure of coating.....	25
3.3	Hardness test .....	26
3.4	Roughness.....	27
3.5	Adhesion test.....	29
3.6	Bending test.....	32
3.7	Impact test.....	33
3.8	Electrochemical porosity test .....	34
3.9	Erosion test.....	37
4	Results.....	39
4.1	Coating microstructure.....	39



4.2	Hardness test .....	47
4.3	Roughness.....	49
4.4	Adhesion test.....	51
4.5	Bending test.....	54
4.6	Impact test.....	57
4.7	Electrochemical porosity test .....	59
4.7.1	OCP measurement .....	59
4.7.2	Current density measurement .....	60
4.7.3	Visual inspection .....	62
4.8	Erosion test.....	67
5	Discussion.....	70
5.1	Microstructure.....	70
5.2	Hardness .....	70
5.3	Roughness.....	71
5.4	Adhesion .....	71
5.5	Bending.....	72
5.6	Impact.....	72
5.7	Corrosion .....	73
5.8	Erosion .....	75
6	Conclusion.....	77
7	Future work.....	78
8	References .....	79
9	Appendix .....	81
9.1	Master thesis assignment text .....	82
9.2	Datasheet for WC-Co (83/17) / NiSF RC 60 50-50.....	84
9.3	Hardness measurements.....	85
9.4	Bending test pictures.....	86
9.5	Adhesion test rupture locations .....	87
9.6	Risk assessment part 1 .....	88

9.7 Risk assessment part 2 ..... 97

## Abbreviations

OCP	Open Circuit potential
HVOF	High Velocity Oxy-Fuel
WC-Co	Tungsten Carbide-Cobalt
NTNU	Norges Teknisk-Naturvitenskapelige Universitet (Norwegian university of science and technology)
kPa	Kilopascal
m/s	Meters per second
µm	Micrometers
Al	Aluminium
Si	Silicon
Ni	Nickel
SEM	Scanning Electron Microscope
HV	Hardness Vickers
IKT	Institutt for Konstruksjonsteknikk (Institute of structural engineering)
MPa	Megapascal
CS	Carbon Steel
NaCl	Sodium Chloride
Ag/AgCl	Silver Chloride reference electrode
PI	Platinum (counter electrode)
Wt%	Weight percentage
Al <sub>2</sub> O <sub>3</sub>	Aluminium oxide (Alumina)
Cr	Chromium
kN	Kilonewton
mA	Miliampere
SiC	Silicon carbide

List of tables

Table 1: Demands of new solution [1] ..... 2  
Table 2: Thermal spray methods..... 6  
Table 3: Key properties obtained by thermal spray methods [4] ..... 6  
Table 4: Abrasive wear coatings [4] ..... 17  
Table 5: Adhesive wear coatings [4] ..... 18  
Table 6: Solid particle erosion coatings [4] ..... 20  
Table 7: Cavitation erosion coatings [4]..... 21  
Table 8: Slurry erosion coatings [4]..... 21  
Table 9: Test used to obtain coating properties ..... 23  
Table 10: Overview of samples for testing..... 24  
Table 11: Proposed erosion test parameters ..... 38  
Table 12: Hardness test measurement ..... 48  
Table 13; Roughness measurements ..... 49  
Table 14: Roughness test parameters..... 50  
Table 15: Adhesion test stress and location of rupture ..... 53  
Table 16: Average tensile strength at rupture ..... 53  
Table 17: Impact energy values..... 57  
Table 18: OCP measurement after 24 hours..... 59  
Table 19: Test parameters for erosion test..... 67  
Table 20: Test results for erosion test..... 69  
Table 21: Hardness measurements for 45 degree spray angle ..... 85  
Table 22: Hardness measurements for 90 degree spray angle ..... 85

## List of figures

Figure 1: Flame spray process [18].....	7
Figure 2: HVOF process [18] .....	8
Figure 3: Detonation gun process [18] .....	9
Figure 4: Plasma spray process [18] .....	10
Figure 5: Wire arc spray process [18].....	11
Figure 6: Cold spray process [16] .....	12
Figure 7: Abrasive wear rate for WC-17Co for HVOF and cold spray [6] .....	14
Figure 8: Abrasive wear rate for WC-12Co for HVOF and cold spray [6] .....	14
Figure 9: Volume loss during abrasion test [6] .....	15
Figure 10: Abrasive wear [19] .....	16
Figure 11: Adhesive wear [19].....	17
Figure 12: Erosive wear [19].....	19
Figure 13: Erosion vs. impact angle [20] .....	20
Figure 14: Galvanic table [21] .....	22
Figure 15: Roughness profiles [11].....	27
Figure 16: Adhesion test adapters .....	30
Figure 17: Test samples with adapters.....	30
Figure 18: Adhesion test setup.....	31
Figure 19: Bending test setup .....	32
Figure 20: Electrochemical porosity test setup.....	35
Figure 21: Erosion test setup.....	37
Figure 22: Microstructure of 45 degree spray at x100 magnification .....	39
Figure 23: Microstructure of 90 degree spray at x100 magnification .....	40
Figure 24: Thickness measuring .....	40
Figure 25: Different phases at high magnification .....	41
Figure 26: Microstructure at 150x magnification. 45 degree spray angle.....	42
Figure 27: Microstructure at 149x magnification. 90 degree spray angle.....	43
Figure 28: Pore in coating at 5220x magnification .....	44
Figure 29: Unmelted phases through the coating .....	45
Figure 30: Microstructure of 45 degree sample .....	46
Figure 31: Soft phase.....	47
Figure 32: Hard phase .....	47
Figure 33: Surface roughness measuring .....	49
Figure 34: Adhesion test for uncoated samples .....	51
Figure 35: Adhesion test for samples coated with 90 degree spray angle .....	52
Figure 36: Adhesion test for samples coated with 45 degree spray angle .....	52
Figure 37: Bending test .....	54
Figure 38: Sample 1 bending test.....	55
Figure 39: Force applied on bending samples .....	56
Figure 40: Support movement during bending test.....	56
Figure 41: Cracks and spalling of sample 1 .....	57
Figure 42: Cracks near edge of impact test.....	58

Figure 43: Cracking pattern for impact test .....	58
Figure 44: Current density 90 degrees .....	60
Figure 45: Current density 45 degrees .....	60
Figure 46: Corrosion test after one month .....	62
Figure 47: Corrosion test samples after test completion .....	63
Figure 48: From left to right: sample 1, 2 and 3.....	63
Figure 49: Peeled surface of sample 2 corrosion test.....	64
Figure 50: Sample 1 cross-section at 50x magnification, degraded coating.....	64
Figure 51: Sample 1 cross-section at 50x magnification, adhesion loss .....	64
Figure 52: From left to right: Sample 1,2 and 3 corrosion test.....	65
Figure 53: From left to right: Sample 4 and 5 corrosion test.....	65
Figure 54: Sample 6 corrosion test.....	66
Figure 55: Sample 1 after erosion test .....	68
Figure 56: Sample 2 after erosion test .....	68
Figure 57: Sample 3 after erosion test .....	69
Figure 58: The four sections of hardness measurement in the coating .....	85
Figure 59: Bending test sample 2 .....	86
Figure 60: Bending test sample 3 .....	86
Figure 61: Bending test sample 4 .....	86
Figure 62: Bending test sample 5 .....	86
Figure 63: Bending test sample 6 .....	86
Figure 64: Bending test sample 7 .....	86
Figure 65: Bending test sample 8 .....	86
Figure 66: Adhesion test sample 3 .....	87
Figure 67: Adhesion test sample 4 .....	87
Figure 68: Adhesion test sample 5 .....	87
Figure 69: Adhesion test sample 6 .....	87
Figure 70: Adhesion test sample 7 .....	87
Figure 71: Adhesion test sample 8 .....	87
Figure 72: Adhesion test sample 9 .....	87
Figure 73: Adhesion test sample 10 .....	87
Figure 74: Adhesion test sample 11 .....	87
Figure 75: Adhesion test sample 12 .....	87



# 1 Introduction

## 1.1 Background

Omya Hustadmarmor is an international company, processing lime for applications in the paper industry. Between the different processing steps, liquid marble is transported in pipes. During this transportation and processing, the marble will contain a considerable amount of coarse particles. The high amount of particles, combined with factors such as grain size and flow speed, is causing concern due to the possibility of abrasive wear in the pipes. High amounts of abrasive wear in the pipes could eventually damage the integrity of the piping system.

To reduce the risk of wear damage in the system, Omya Hustadmarmor have applied pipes in a stainless steel alloy, with an internal ceramic coating. This gives a more wear resistant solution, but there are several drawbacks connected with this:

- The pipes gain a considerable amount of weight, causing disadvantages in the assembly of the pipes.
- The ceramic coating has a thickness of 25mm, which means the stainless steel pipes must be made larger to compensate for the extra thickness.
- The piping has proved to be weak against external forces, which causes cracking of the ceramic coating.
- For some applications, the ceramic coating has limited wear properties due to the coating binder being torn off.

On this background, Omya Hustadmarmor took part in a project, «Korrosjons- og slitasjebestandig beskyttelse av glatte metallflater». This project is carried out in cooperation with Norges Forskningsråd, Brunvoll, Aquamarine Subsea, Triplex, SINTEF and NTNU. The essence of this project is to develop new machining processes, fabrication processes and innovative uses of thermal spraying to improve corrosion and erosion resistance of smooth surfaces. Thermal spraying in pipes is one of the main activities of this project.

This activity has an objective of creating an internal pipe surface, which provides the necessary protection against corrosion and erosion. The life cycle cost of this new solution should be lower than what is currently the case today.



## 1.2 Development of a new solution

To improve the existing solution of corrosion and erosion protection, the demands listed in Table 1 needs to be fulfilled:

**Table 1: Demands of new solution [1]**

Main requirement	Create a piping surface that reduce corrosion and erosion to the extent that a lifetime of 15 years is provided for a complete piping system with internal diameter of 100mm and larger. This includes pipes, corners, t-pipes and concentric transitions.
Requirement of method	<ul style="list-style-type: none"> <li>• Prioritize use of thermal spraying to apply the coating</li> <li>• The chosen method of thermal spraying must be applicable for pipe fittings described</li> <li>• Obtain methods of pre-treatment, which provides desired properties of coating</li> <li>• Develop method and equipment, which allows for internal thermal spraying of pipes</li> <li>• A minimum length of 3 meters of the pipe must be coated, which means 1,5 meters on both sides</li> <li>• Wall thickness of pipes is 2mm and more</li> </ul>
Requirements of coating	<ul style="list-style-type: none"> <li>• Maximum coating thickness of 1000<math>\mu</math>m (1mm). This requirement can be revised if there is a higher demand of robustness of the coating</li> <li>• The coating must withstand external forces without cracking</li> <li>• Corrosion resistance equal to or better than current solution</li> <li>• Compatible thermal properties between coating and substrate material. This is to prevent stresses in the transition area of the coating and substrate material</li> <li>• The coating is not to discolor the products flowing through the pipe</li> </ul>
Desired, but not demanded properties of the coating	<ul style="list-style-type: none"> <li>• The coating is able to be maintained/repared</li> <li>• Condition monitoring of coating without production stop</li> </ul>
Requirements of the solution in total	<ul style="list-style-type: none"> <li>• Life cycle cost of new solution to be lower than today</li> <li>• Provide a weight reduction of the system compared to current solution</li> <li>• Standarize the complete solution through use of standard pipe dimensions according to ISO and metric system</li> </ul>

Three different types of thermal spray were found relevant to use to cover these requirements. In order to determine which to choose for the project, a variety of resulting properties for the coating were evaluated:

- Amount of heat input to material
- Available equipment for applying the coating
- Porosity of coating
- Adhesion of coating
- Cost of application

With all of the requirements specified in mind, HVOF became the selected method of thermal spray. The evaluation of this method proved it to be more expensive and slower compared to its alternatives, but with a better result regarding the coating properties. As for the composition of the coated material, an Amperit 560 coating was selected. This is a blended coating, which consists of WC-Co (83/17) and Ni-SF RC 60. See appendix 9.2 for a complete datasheet of the Amperit 560 coating. This type of coating is widely used for corrosion and erosion protection of equipment.

### 1.3 The environment experienced in the pipes

The pipes for this project are transporting liquid marble. Coarse particles in the marble have previously been causing erosion of the internal surface of the pipes. The coating for the new solution will have to provide more or equal amount of durability as the previous ceramic solution against these erosion effects.

A thermally sprayed coating will normally have a thickness in the order 0,2-0,4mm. The lifetime of the coating is set to 15 years. This means there are little room for erosion of the coating over time. Small microstructural errors in the coating may compromise the total erosion resistance and cause failure before the expected lifetime. This sets high demands to the spray parameters and the quality of the coating.

The possibilities of corrosion attacks present in such systems will have to be determined as well. Pores and microstructural errors in the coating can allow corrosive media to reach the substrate material. Depending on the corrosivity of the penetrating media, corrosion on the substrate may occur. As the Amperit 560 coating is a metallic coating, there may be some galvanic interaction between the coating and the substrate material. The least noble material will be sacrificed, and for both the coating and the substrate, this will be detrimental to the integrity of the pipe. Corrosion of the substrate will reduce the thickness of the pipe, and not provide the required strength for the system. Corrosion of the coating will reduce the total lifetime of the coating and eventually expose the substrate to the erosion effects present.

Eventual galvanic interactions present and the severity between an Amperit 560 coating and substrate material of carbon steel or stainless steel is not the scope of this report, and will have to be researched separately.

## 1.4 Challenges regarding internal spraying of pipes

Spraying methods that utilize high velocities all require long spraying nozzles to accelerate the powder to a sufficient value. These methods include detonation gun, HVOF and cold spray. The long nozzle of the equipment, in combination with a spraying distance of 100-300mm provides some limitations of these thermal spray methods [2]. Spraying of an internal surface of a pipe is challenging with respect to space needed for the equipment. Pipes with diameter ranges of 100-600mm are used by OMYA Hustadmarmor and will have problems to be sprayed by conventional thermal spray equipment. The size requirements demand more space than the internal diameter of the pipe allows. The optimal spray angle of 90 degrees and spray distances will be hard to achieve in such pipes. This project focuses on the development of equipment and spraying methods able to produce coatings with an acceptable quality in such narrow pipes.

## 1.5 Purpose and composition of report

The selected method and composition of coating will need to undergo comprehensive testing to become the approved solution. To demonstrate how the actual coating responds to the demands and criteria that have been specified, a set of relevant tests are proposed. This report describes the tests carried out to qualify the coating, along with the obtained results from each test.

The report is divided into several parts, each describing relevant matters of this project.

Chapter 2 contains a theory part regarding thermal spraying. Different methods of thermal spray and their supplied properties will be briefly described, with a more thorough look at HVOF and the cold spray method whereby HVOF have been used as the thermal spray method for the coating tested in this project. Cold spray is a relatively new method, which are currently on the research stage, but with promising results. Coating compositions and the properties they provide to the surface will also be presented in this chapter.

Chapter 3 discusses the testing methods used for this research. Relevant theory along with a description of the execution of the test is provided as well.

Chapter 4 is where the actual testing results are being presented, along with an explanation of what information the results provide. Graphs, tables and pictures that describes the results are used where appropriate.

Chapter 5 includes a discussion about the results obtained. Any sources of error that may have affected the results, and if the test uncovered the desired data, are subjects that will be included in this chapter.

## 2 Thermal spraying

Thermal spraying is a term describing a group of coating processes. These processes are recognized by the deposition of molten or semi molten particles that are accelerated towards a surface to form a coating. The feedstock material can be metallic or non-metallic and depending on the type of thermal spraying, the material can be in the form of powder, ceramic rod, wire or molten materials.

There exists a wide variety of techniques for thermal spraying, and they provide different properties to the resulting coating. However, in general they create the coating in the same way. The feedstock material is melted to a molten or semi molten state in a spray gun and atomised using compressed gas to form a spray of droplets. The droplets are deposited on the target substrate to form a coating. Due to the nature that the droplets splat on the substrate, this will form a coating with a lamellar structure.

The amount of heat input and velocities of the particles will determine the amount of deformation of the spray particles. High deformation usually means denser coatings and is achieved by high heat input and high velocity. A low rate of deformation gives a more porous coating.

## 2.1 Methods of thermal spray

As mentioned earlier, there is a wide variety of methods used for thermal spraying. They work a bit differently regarding the method of heating the feedstock material and may thus be separated in different groups. See Table 2 for classification of the different groups.

**Table 2: Thermal spray methods**

Thermal spray			
Combustion	Detonation	Electrical	Cold spray

The four methods presented in Table 2 is a common way of separating the different techniques regarding the heat source. The category labelled detonation is a combustion process, but considered a separate category as this technique works a bit differently than the other combustion processes. Each of the presented methods are further split up into different sub-methods and will be presented more closely in the chapter 2.1.1, 2.1.2, 2.1.3 and 2.1.4.

Some key properties to the different methods are presented in Table 3.

**Table 3: Key properties obtained by thermal spray methods [4]**

Process	Temperature [°C]	Particle Velocity [m/s]	Adhesion [MPa]	Oxide content [%]	Porosity [%]	Relative cost (a)	Thickness [mm]
Flame Powder	3000	40	8	10-15	2-6	1	0.1-15
Flame Wire	4000	100	12	10-20	10	2	0.1-15
HVOF	3000	800	>70	1-5	1-2	3	0.1-2
D-Gun	4000	800	>70	1-5	1-2	4	0.05-0.3
Electric Arc	5000	240	>60	5-10	5	1	
APS	12000	200-400	10-70	1-3	1-5	4	0.1-1
VPS	12000	400-600	>70	0	<0.5	5	0.1-1
Cold Spray	<500	550-1000	20-70	0	<0.5	3	0.1-2

(a) 1 (low) to 5 (high)

### 2.1.1 Combustion

In a combustion spray technique, the method of heating is a constant flame usually created by a mixture of oxygen and acetylene. The feedstock material is transported through this flame to be heated. Compressed air then propels the spray droplets to the surface to form a coating.

#### 2.1.1.1 Flame spray

The flame spray process is a simple and cheap method of thermal spraying. Compared to other methods, it utilizes lower temperatures and velocities and thus producing a more porous coating with lower densities and adhesion strength. The feedstock of flame spray can be powder or wire, but the behaviour in the flame spray gun is the same for both of them. Flame spray can be used for all metals that melts below the flame temperature of 3000-4000°C. Figure 1 gives a presentation of how the flame spray operates. Oxygen and fuel is ignited to make a continuous flame, where feedstock material is heated and accelerated by atomising air. Even though flame spray produces coatings with worse properties than other methods, it may be good for some applications. For instance, this can be zinc or aluminium sprayed on a surface to provide cathodic protection. As these metals will act as a sacrificial anode, there is not a demand that they are free of pores. However, a coating of a metal that is cathodic to the surface needs a pore-free coating to achieve its effect, as mentioned in chapter 2.3.2.

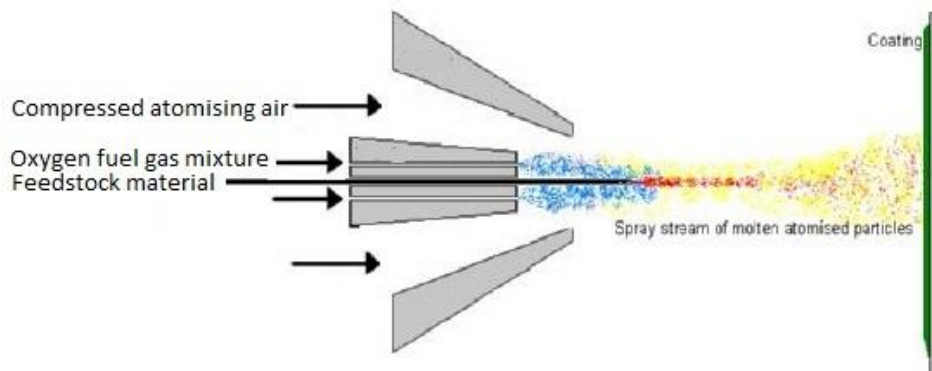


Figure 1: Flame spray process [18]

### 2.1.1.2 HVOF

HVOF (High velocity oxy-fuel) is another type of combustion spray. The temperature and heating method is the same as for flame spray, except that HVOF uses a much higher velocity of the spray stream. There are numerous types of HVOF guns to produce the high velocity required. One type is presented in Figure 2. This shows a combustion chamber where fuel and oxygen are fed. When this mixture is combusted, it causes a high pressure flame stream that is forced down a long nozzle with a high velocity. Powder is mixed with the flame stream and this causes an increased velocity compared to flame spray. Despite the low particle temperature, high density coatings are still achieved through high particle impact velocity. This means that particles do not need to be molten to form a high quality coating, as the high impact energy will deform unmolten particles. Particle heating in the form of transformation of kinetic energy to thermal energy during the impact will also aid the production of dense coatings.

The HVOF process is well known to produce high quality hard cermet coatings, such as WC-Co. As the WC-Co coating is exposed to high temperatures during deposition, there is a small amount of decarburisation and dissolution of carbides [3]. Formation of brittle  $W_2C$  and Co-W-C are the consequences of this and affects the mechanical properties for the coating. The amount of decarburisation and dissolution of the carbides are still much lower than experienced from plasma spray, as the temperature during spraying are much lower [4].

The combustion fuel gases used for the HVOF process are usually hydrogen, propylene, kerosene, propane or acetylene. There are two distinct classes of HVOF spray devices, which are divided according to the combustion fuel used and the chamber pressure. The first class, high velocity, have chamber pressures exceeding 241kPa. The second class, hyper velocity, has chamber pressure in the range of 620 to 827 kPa and is typically fuelled with kerosene. High combustion chamber pressures have a tendency of producing coatings with compressive stresses, which is usually beneficial for the function of a coating. However, the deposition efficiency of the hyper velocity kerosene guns will suffer compared to the lower pressure guns. The deposition efficiency for conventional HVOF guns is in the range of 50-70%, while kerosene guns is in the range of 35-50%.

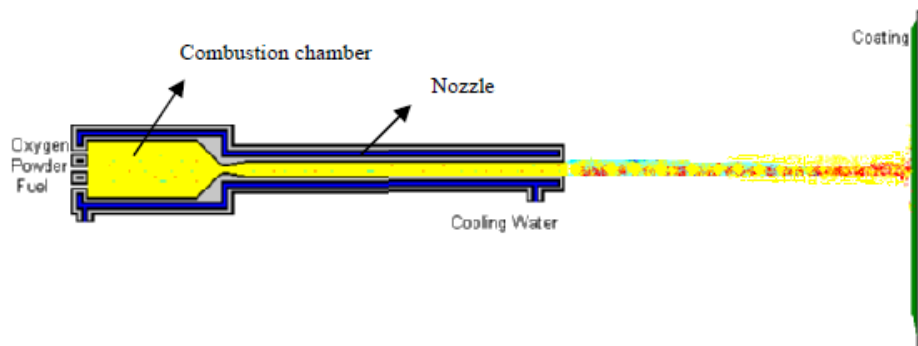


Figure 2: HVOF process [18]

### 2.1.2 Detonation

The detonation process is a combustion process, but works a bit differently. While the combustion process provide a steady flame where particles are continuously transported, the detonation process is more of a pulsating process. As illustrated in Figure 3, powder is fed into a chamber along with oxygen and fuel, and ignited by a spark. The combustion transports the mixture though a long barrel to the substrate as a gun shot. This process achieves even higher velocities than experienced for HVOF and creates high density, low porosity coatings with high bond strength. The downside with the detonation method, is the large barrel required. Substrates in narrow spots will be hard for the detonation gun to properly coat. Nitrogen is used to purge the barrel between each shot. The cycle of purging, injection and ignition occurs with a frequency between 3 to >10 times per second [4].

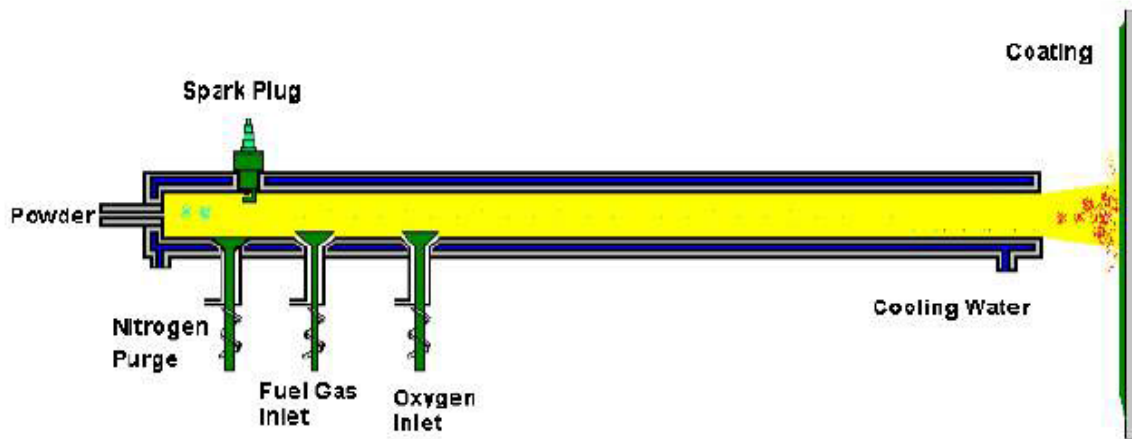


Figure 3: Detonation gun process [18]



### 2.1.3 Electrical spray

#### 2.1.3.1 Plasma spray

Plasma spray uses electrical energy to create a plasma flame for heat input. This causes a very high heat input on the particles combined with a high velocity gas stream. The plasma can reach temperatures up to 15000°C, which is above the melting temperature for most of the materials known. The high degree of melting combined with a high velocity gives coatings with a high density and bond strength. Using inert gases in the plasma stream have proven to give a significant reduction of the oxide content in the coating. There are two types of plasma spray; atmospheric plasma spray and vacuum plasma spray. Vacuum plasma spray is performed with an absence of oxygen. This gives a coating with a lower amount of oxidation, in addition to generally better coating properties. However, the vacuum type is more expensive compared to atmospheric type.

The plasma gun is composed of a copper anode and a tungsten cathode, and is illustrated in Figure 4. Plasma gas flows through the cathode to the anode, which is shaped as a constricting nozzle. A high voltage discharge forms a current arc between the anode and cathode. When plasma gas flows through this arc, the resistance heating will cause the gas to reach extreme temperatures and ionize. This ionized gas will become plasma and work as a heat input for the feedstock powder. The spray velocity is higher than flame spray, but lower than HVOF and detonation gun. Still, due to the high amount of molten particles, the coating quality is good, with properties comparable to HVOF and detonation spray.

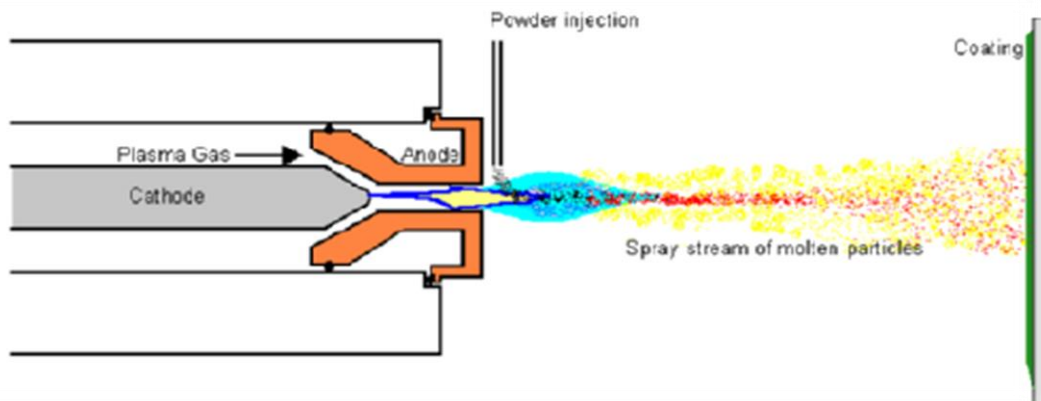


Figure 4: Plasma spray process [18]

### 2.1.3.2 Wire arc spray

A wire arc spray uses electrical energy as a heat source, but in another way than what plasma spray utilizes. This method uses two wire electrodes that are advanced to a common point, where they touch. The composition of a wire arc gun is illustrated in Figure 5. A potential difference applied in the wires will initiate an arc when the tips meet, and will cause them to melt. A gas, usually argon is then used to further atomise the particles and accelerate them to the substrate surface. The coating properties gained by this technique are not the best, but it is relatively cheap and easy to perform. It will contain some porosity and oxides, but provide good adhesion.

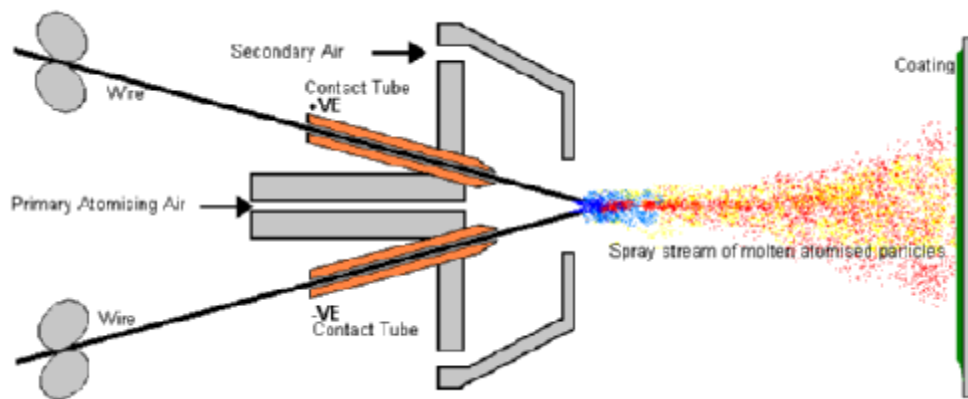


Figure 5: Wire arc spray process [18]

#### 2.1.4 Cold spray

Cold spray is a relatively new method compared to the other techniques. Its use has not been adapted in the industry as much as the more known techniques. The process of cold spray is quite different compared to the other methods. While the other presented techniques utilizes temperatures in the range of several thousand degrees, the cold spray technique experiences temperatures in the range of about 100-500°C. As the temperatures are rather low, the powder feedstock used for cold spray will not reach a molten state. The case for cold spray is that it utilizes extreme velocities to achieve good coating properties, even higher velocity than detonation or HVOF technique. The velocity used depends on feedstock material, but can be in the range of 1000 m/s. Because of this high velocity, the particles will deform on a substrate to form a coating even if they are not molten.

A typical system for cold spray is showed in Figure 6. High pressure gas is introduced through a gas control module to a gas heater and powder feeder. Unlike the other methods presented for thermal spraying, the gas is not heated to melt the feedstock powder. The gas is heated to achieve higher flow velocities as high temperature gas will expand and increase pressure. The heated gas is used to accelerate the powder to the high velocities needed. Just as with detonation and HVOF, there is a long nozzle used to accelerate the gas and powder mixture.

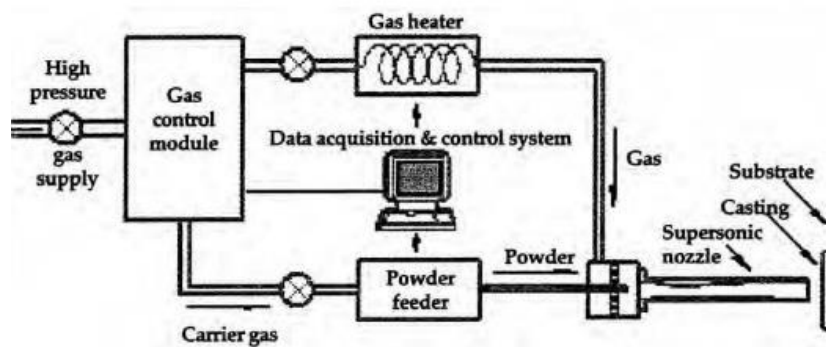


Figure 6: Cold spray process [16]

The gases used are air, nitrogen or helium. Air is the cheapest of these three gases, but with the disadvantage of producing oxidation in the coating. The most used is Nitrogen as this is relatively cheap and keeps oxidation at a minimum. For some applications, the velocities produced by the use of nitrogen is not sufficient to produce coatings with the desired properties. Helium is used for these applications as it is capable of reaching the highest velocities of the three gases. However, Helium is more expensive than nitrogen and a mixture of these are often used to improve the economical aspect of the process. Gas handling systems to recycle the helium gas have been developed in an attempt to further improve the cost of using Helium.

There are some drawbacks to use cold spray. Hard, brittle materials can not be sprayed using cold spray, and will require a ductile binder blended with the sprayed powder. In addition, due to the extreme velocities achieved using cold spray, it may damage some substrate surfaces [5]. These substrates will suffer from the high kinetic energy of the coating particles.

## 2.2 Comparison of HVOF and cold spray method

Both the HVOF and cold spray method provide coatings of high quality. The HVOF utilizes a combination of high temperature and high velocity to obtain the good properties. Cold spray relies on extreme particle velocities to make particles plastically deform, without any significant heat input. These parameters will affect different aspects of the coating.

As mentioned in chapter 2.1.1.2, the carbides of a WC coating will suffer under high temperatures to create brittle W<sub>2</sub>C and Co-W-C phases. Thus meaning a reduction of heat input to the spray powder could cause even lower amount of decomposition of the carbides. A report released in 2014 focuses on this matter, where coatings of WC-17Co and WC-12Co were produced both using HVOF and cold spray [6]. Analysis of the resulting coatings obtained showed that there were no presence of W<sub>2</sub>C or Co-W-C for the cold sprayed coating, but some amount for the HVOF coating. This resulted in a higher hardness and lower ductility for the HVOF coating as the decarburisation phases are harder, with a consumption of the ductile Co phase.

Both of the surfaces were subjected to abrasion tests to compare the wear resistances provided. This test consisted of a rubber ball sliding along the coated surface. The resulting wear rates measured is visualized in Figure 7 and Figure 8. Both of the coating types gave good results on wear resistance, but with a slight improvement for the cold sprayed coating. The increased initial wear rate is due to surface roughness of the coating. As the roughness peaks are worn off, the total wear rate stabilizes at a lower rate.

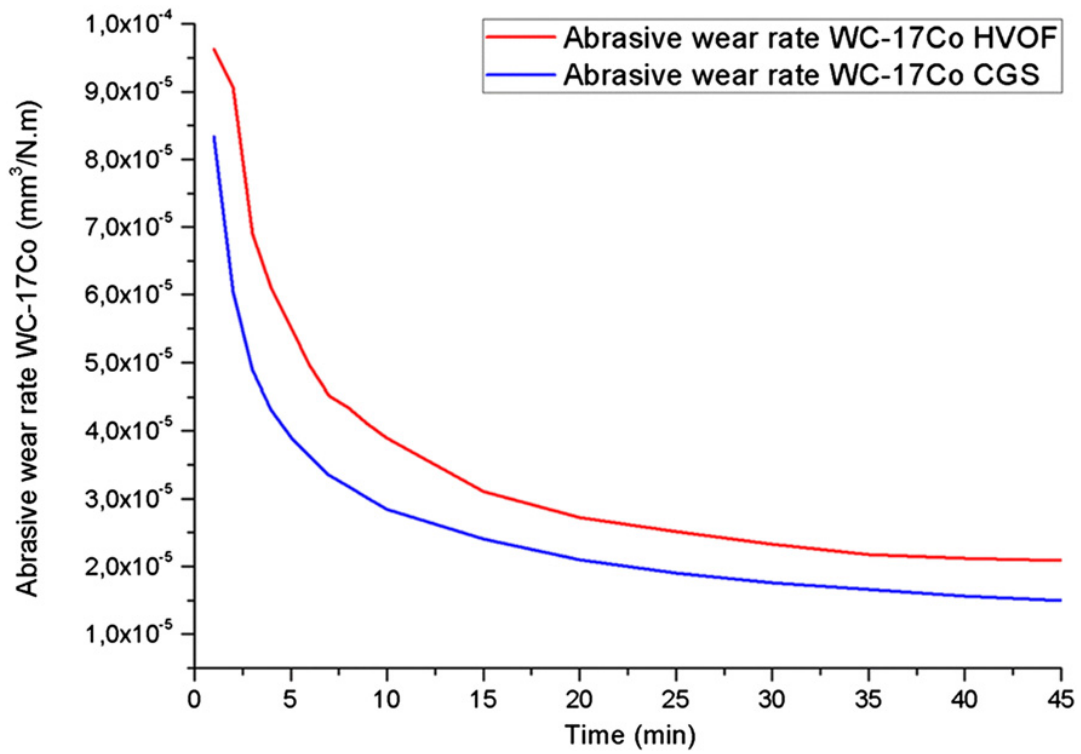


Figure 7: Abrasive wear rate for WC-17Co for HVOF and cold spray [6]

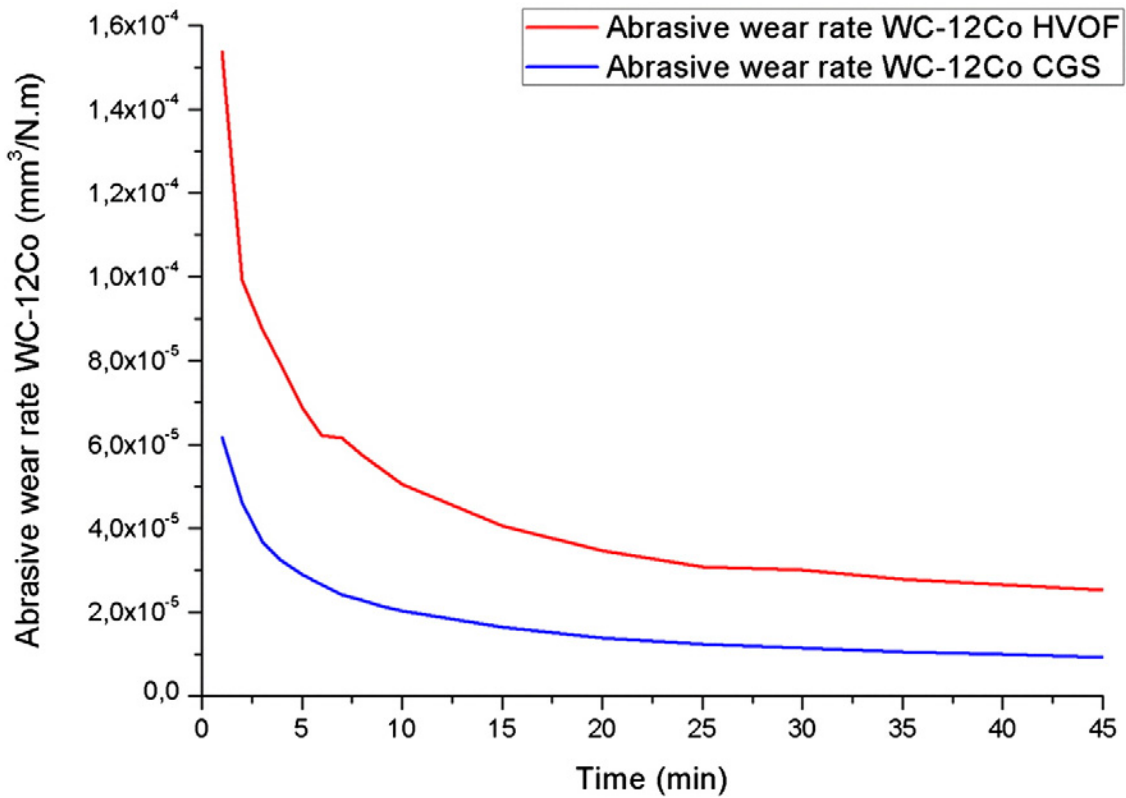


Figure 8: Abrasive wear rate for WC-12Co for HVOF and cold spray [6]

This may indicate how the presence of the decomposed carbides will affect the coating. The total volume loss during the abrasion wear test is presented in Figure 9. There is a clear difference between the cold sprayed coatings compared to HVOF for both of the WC-Co coatings.

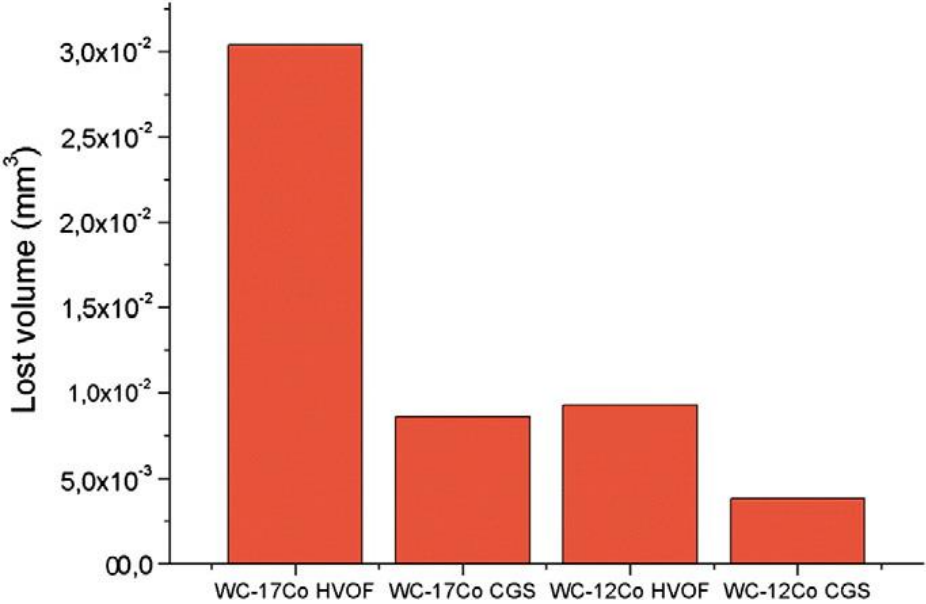


Figure 9: Volume loss during abrasion test [6]

The cold spray deposition method relies on cold working of the particles to form a coating. A high amount of cold working on a metal will make it harder, but at a cost of reduced ductility. Because of this, the cold spray method typically gives coatings with a reduced ductility, compared to the methods that gives higher heat input to the particles, like HVOF [4]. This gives a more brittle coating with higher tensile strength. However, if the coating is subjected to any deformations, the probability of crack initiation increases.

## 2.3 Coatings

Thermal sprayed coatings have a wide variety of uses. Different compositions and spray method of the coatings will all provide different results. One coating composition may be perfect suited for one application, but not be sufficient for another. Applications of thermal sprayed coating include:

- Wear resistance
- Thermal insulation
- Corrosion resistance
- Lubrication or low friction surfaces
- Electromagnetic shielding

The main requirement of the new coating solution for this project was to provide corrosion and wear resistance to a steel pipe, see Table 1. The mechanics of these challenges will be described in the following chapter along with a short description on which coatings that may protect against the different mechanics.

### 2.3.1 Wear resistance

The selection of a coating for wear resistance requires an understanding of the different wear mechanisms, as there are more than one. While the general term of wear means loss of material, there are several different ways this will occur on a material surface, and will have different demands on how the coating protects the surface.

#### 2.3.1.1 Abrasive wear

The term abrasive wear is the wear mechanism that occurs when two surfaces are sliding relatively to each other. A two-body abrasive wear is roughness peaks on a hard surface that scratches the softer surface. A three-body wear is hard, free flowing particles occurring between two sliding surfaces. These hard particles rotate or slide between the two surfaces to cause wear. See Figure 10 for illustrations of these wear mechanisms.

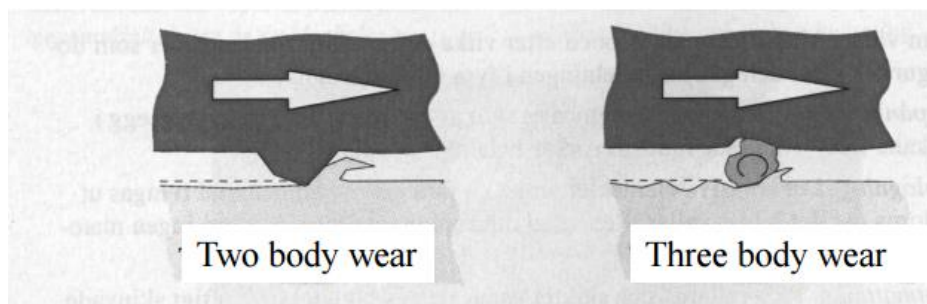


Figure 10: Abrasive wear [19]

Some thermally sprayed coatings, such as the Amperit 560 coating contains hard particles in a softer matrix. The softer matrix in such coatings will be more susceptible to wear than the harder phase. The consequence of high wear rates in the soft matrix is that the hard phases will lose support and fall off. The abrasion resistance of such coatings will improve with a high concentration and low size of hard particles. In this way, there will be an even distribution of hard phases in the coating, not leaving large areas of soft matrix exposed, and thus provide better overall abrasion resistance.

Examples of coatings to protect against abrasive wear are listed in Table 4.

**Table 4: Abrasive wear coatings [4]**

Material family	Composition
Ceramics (oxides)	$Cr_2O_3$ , $Al_2O_3$ , $TiO_2$ (mixtures thereof)
Cermet (carbide) composites	WC/Co, WC/Co/Cr, WC/Ni, WC/NiCr, WC/ $Cr_3C_2$ /Ni/NiCr, WC/NiCrSiBC (fused), $Cr_3C_2$ /NiCr
Metallic alloys	NiCrSiBC(b) (fused), CoNiCrSiB (fused), CoCrW(b), CoCrMo(b), CoCrMoSi, CoCrNiW(b), FeCrMo

**2.3.1.2 Adhesive wear**

Adhesive wear occurs between two surfaces sliding relatively to each other, in the same way as abrasive wear. However, the mechanism between the two is a bit different. When two materials slide against each other with high force, this may cause cold welding between the two surfaces. This will cause a small local adhesion effect in the contact zone. Movements between the materials will cause a high shear force and the weakest material will start to fracture and be torn from the surface. This mechanism is illustrated in Figure 11.

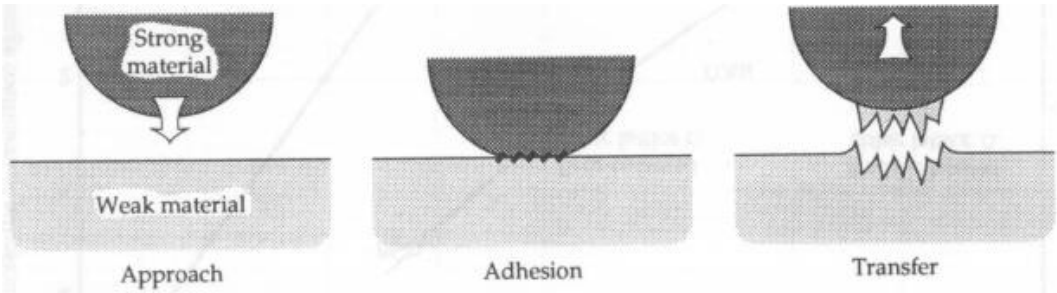


**Figure 11: Adhesive wear [19]**



Examples of coatings to protect against adhesive wear is listed in Table 5.

**Table 5: Adhesive wear coatings [4]**

<b>Material family</b>	<b>Composition</b>
Ceramics (oxides)	Cr <sub>2</sub> O <sub>3</sub> , Al <sub>2</sub> O <sub>3</sub> , Al <sub>2</sub> O <sub>3</sub> -TiO <sub>2</sub>
Cermet (carbide) composites	WC/Co, WC/Co/Cr, WC/Ni, WC/NiCr, WC/Cr <sub>3</sub> C <sub>2</sub> /Ni/NiCr, WC/NiCrSiBC (fused), Cr <sub>3</sub> C <sub>2</sub> /NiCr
Metallic alloys	Mo, Mo/NiCrSiB, CoCrMoSi  420SS, Al bronze, Babbitt, Sn  NiCrSiBC (60 RC fused)  CoCrMoSi CoCrW, CoCrMoW(b), FeMoCr

### 2.3.1.3 Erosion

Erosive wear describes the mechanism of material loss due to particle impact on a surface. High impact forces on hard particles may remove mass on a surface by repeatedly striking the surface over time. Impact speed and velocity will all affect the erosion mechanism and the reaction of the material. We can split the erosion wear mechanisms into six different types, where the assigned letter corresponds to Figure 12:

- a) Abrasion at low impact angles
- b) Surface fatigue during low speed, high impact angle
- c) Brittle fracture or multiple plastic deformation during medium speed, high impact angle
- d) Surface melting at high impact speed
- e) Macroscopic erosion with secondary effects
- f) Crystal lattice degradation from impact by atoms

See Figure 12 for illustrations of the six erosive wear types.

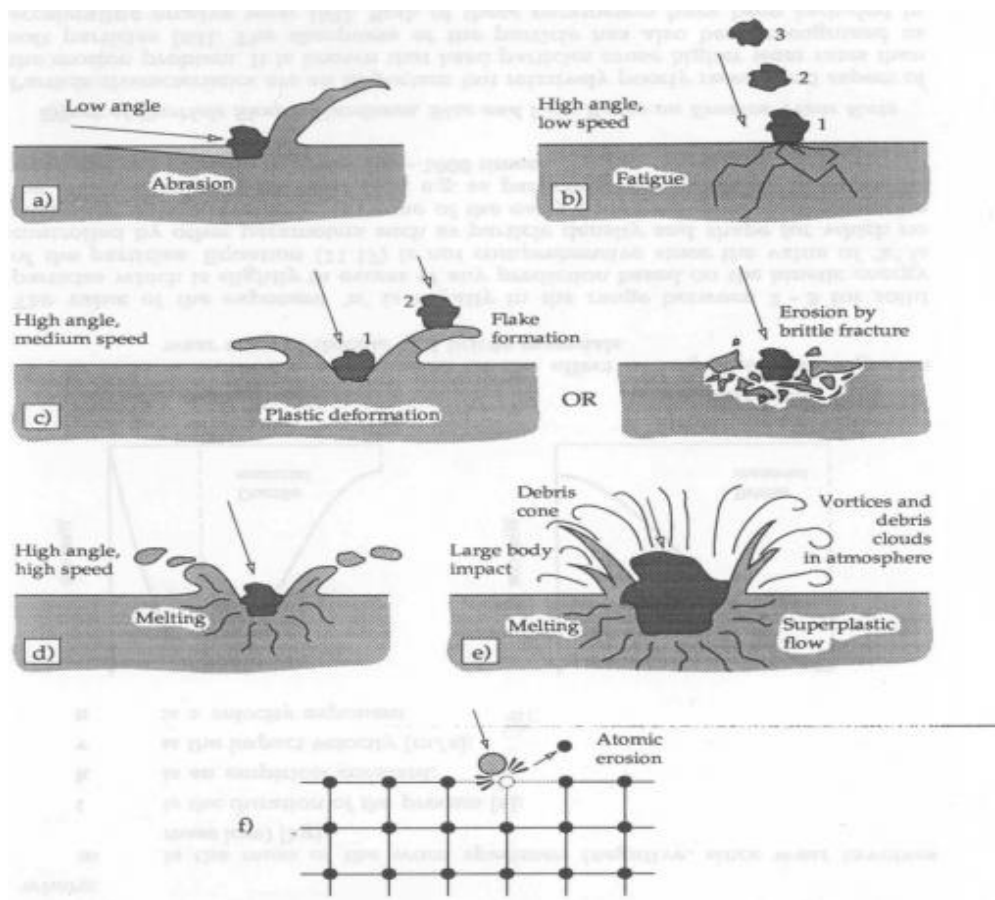


Figure 12: Erosive wear [19]

All of these are highly dependent of the particle characteristics, but also on the material properties. The amount of erosion will have a high dependency on the relation between ductile/hard materials and low/high angle of impact. A particle of low impact angle on a substrate will have a high erosion effect on a ductile material, but low erosion rate on a hard material. The erosion effect with low angles is abrasion as described above, and the ductile material will experience a plowing effect from the particle. The particle impact on the hard material will do much less damage due to the increased abrasion resistance a hard material experiences. The effect will be opposite for particles with a high angle of impact. While the hard material will be more susceptible to brittle failure of the surface, the ductile material will experience a higher degree of bouncing effect on the particle. From these conditions, a relation between erosion rate and impact angle can be presented as in Figure 13.

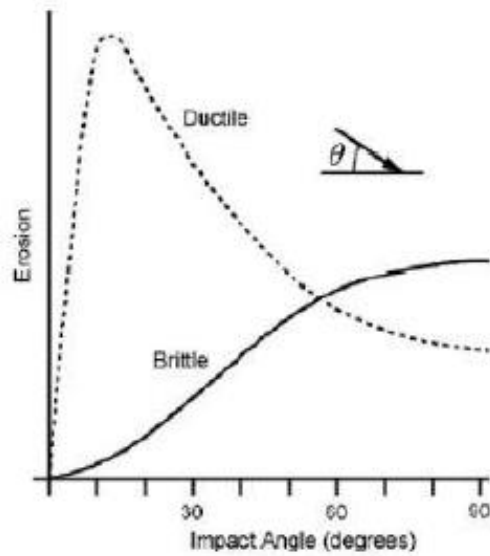


Figure 13: Erosion vs. impact angle [20]

There are four distinct types of erosive wear [4]:

- Dry solid particle erosion
- Liquid droplet erosion
- Cavitation erosion
- Slurry erosion

Dry solid particle erosion is repetitive impingement of solid particles on a surface. The amount and effect of erosion wear is determined by the properties of the coating and for the striking particles. Examples of coatings used to protect against solid particle erosion are listed in Table 6.

Table 6: Solid particle erosion coatings [4]

Material family	Composition
Ceramics (oxides)	$\text{Cr}_2\text{O}_3$ , $\text{Cr}_2\text{O}_3\text{-Al}_2\text{O}_3$ , $\text{Cr}_2\text{O}_3\text{-TiO}_2\text{-SiO}_2$
Cermet (carbide) composites	WC/NiCrSiBC (fused), $\text{Cr}_3\text{C}_2\text{/NiCr}$ , WC/Co, FeCrMo, WC/CoCr
Metallic alloys	NiCrSiBC(b) (fused), CoNiCrSiB (fused), CoCrMoSi, FeCrMo, FeCrAl (Y), nickel/high-chromium/carbon alloys

The liquid droplet erosion is caused by shock waves introduced by liquid drops striking the surface. This causes fatigue of the surface, and can over time lead to spalling or pits in the coating.

Cavitation erosion is caused by collapse of air bubbles in a liquid flow system. This usually occurs when there are rapid pressure changes in the system. The bubbles can implode near the coating surface and cause shocks of cyclic stress. This can eventually cause fatigue of the surface and wear. Examples of coatings used to protect against cavitation are listed in Table 7.

**Table 7: Cavitation erosion coatings [4]**

Material family	Composition
Ceramics (oxides)	...
Cermet (carbide) composites	CoCr-WC
Metallic alloys	NiCrSiBC(b) (fused), CoNiCrSiB (fused), CoCrW(b), Al bronze, CuNi

Slurry erosion is particles in a fluid flow that strikes the surface. This exposes the surfaces to the same mechanics found in dry particle erosion. However, as this is a fluid flow, there may be corrosive effects present. The coating needs to protect against both erosion and corrosion. Examples of coatings used to protect against slurry erosion are listed in Table 8.

**Table 8: Slurry erosion coatings [4]**

Material family	Composition
Ceramics (oxides)	Cr <sub>2</sub> O <sub>3</sub> , Al <sub>2</sub> O <sub>3</sub> -TiO <sub>2</sub>
Cermet (carbide) composites	WC/Co, WC/Co/Cr, WC/NiCrSiBC (fused), WC/CoNiCrSiB (fused)
Metallic alloys	NiCrSiBC(b) (fused), CoNiCrSiB (fused)

### 2.3.2 Corrosion resistance

Corrosion protection by the use of coatings is done with two different types of coatings, sacrificial and non-sacrificial coatings. These two types will both protect against corrosion, but the theory behind them is a bit different.

A sacrificial coating, as the name implies, sacrifices itself to prevent corrosion of the substrate. This requires the coating to have a cathodic behaviour compared to the substrate material. The behaviour between different materials is found in a galvanic table, which lists different materials in their order of nobility. A less noble material will be sacrificed for a more noble material in the presence of metallic contact and an electrolyte. From the galvanic table from Figure 14, zinc and aluminium is listed as the least noble materials. This means these will sacrifice itself to protect all the other materials in the table. Due to their availability and price, they are also the most used materials used for sacrificial coatings. These coatings do not rely on a low porosity of the coating, as they will protect the substrate even if water or other corrosive media penetrate the coating. Aluminium and zinc are relatively soft materials, which mean they will not provide any protection against wear.

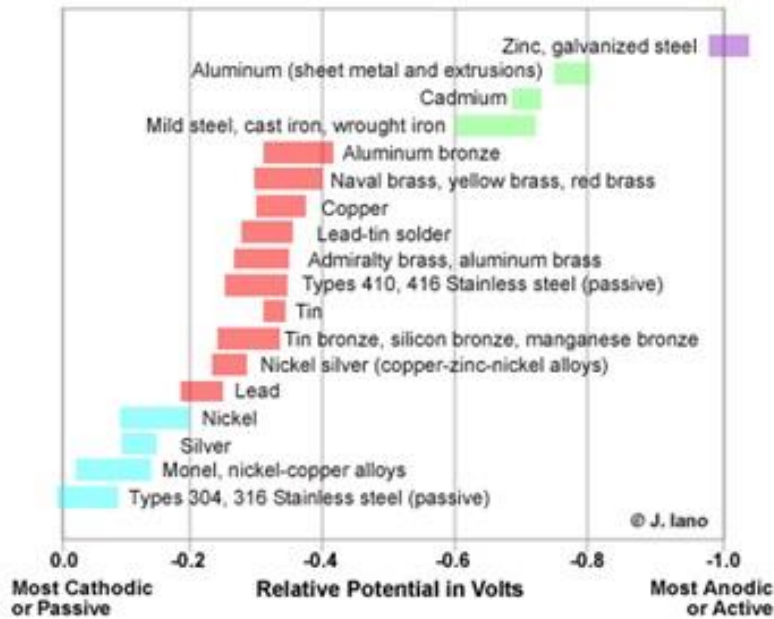


Figure 14: Galvanic table [21]

A non-sacrificial coating will not sacrifice itself to protect the substrate, and will usually be cathodic compared to the substrate. Even if the coating is cathodic to the surface, corrosion will not initiate unless the electrolyte reaches the substrate. If this happens however, the substrate will be sacrificed to protect the coating, which is not favourable and will accelerate the corrosion rate. This means the purpose of these coatings is to prevent any corrosive media to reach the substrate surface. This gives a higher demand of lower porosity than the sacrificial coatings. Small cracks in the coating that exposes the substrate material will be enough to initiate corrosion, and unless corrosion products plug the crack, the corrosion will continue. Non-sacrificial coatings are often used to protect against corrosion and wear, and thus usually have a higher hardness compared to the sacrificial coatings. The Amperit 560 coating used in this thesis is a coating of this type, and have exceptional properties against wear. As long as the coating remains intact and free of pores, the coating will protect against corrosion attacks as well.

### 3 Testing

The tests listed in Table 9 are used to obtain data of the coating properties.

**Table 9: Test used to obtain coating properties**

<b>Test</b>	<b>Purpose</b>
Microscopical analysis	Examine the microstructure of the coating to reveal pores and faults present
Hardness	Measure hardness of the coating to confirm quality and compare values to standard Norsok M-630 [7].
Roughness	Measure roughness of the surface of the coating. Compare results to proposed roughness in standard Norsok M-630 [7].
Adhesion	A test to confirm if the coating properly adhere to the substrate using test method proposed in ASTM C633 [8]. Compare results to standard Norsok M-630 [7].
Bending	Bend coated samples to observe coating behaviour under deformation. Compare results to acceptance criteria in Norsok M-630.
Impact	Weight drop on coating to observe coating behaviour under shock conditions. Use standard ISO 6272-1-2011 [9]
Corrosion	Polarise coated samples subjected to seawater and measure how well the coating prevents corrosion on the substrate. Use test procedure proposed in DNV C2 [10]
Erosion	Samples are sprayed with a water/sand slurry over time to check how well the coating resists erosive effects.

#### 3.1 Samples for testing

For the testing, wide varieties of test samples are supplied. The coating used on the test samples are Amperit 560. However, the spray condition differs. For all tests, samples with both spray angle 45 degrees and 90 degrees are supplied. By comparing test results of these two spray conditions, the better solution may be qualified.

A complete list of samples used on testing and characterization of the coating is listed in Table 10 below. These tests are performed to qualify the coating regarding the specification of demand [1].

**Table 10: Overview of samples for testing**

<b>Number</b>	<b>Test method</b>	<b>Number of samples</b>	<b>Description</b>
1.	Microstructure	1 of 45, 1 of 90	The cross section of coating will be observed in optical microscope and SEM. In addition, the elemental distribution in the coatings will be characterized in XRD.
2.	Hardness	1 of 45, 1 of 90	The cross sectional side of the coating will be tested for hardness values
3.	Roughness	1 of 45, 1 of 90	
4.	Adhesion tensile test	5 of 45, 5 of 90, 2 uncoated	Coated and uncoated samples will be glued together and subjected to tensile strength to measure the fracture force required.
5.	Bending test	5 of 45, 3 of 90	Coated plates will be bent over a mandrel to examine the coating behaviour under deformation.
6.	Impact test	Edges from samples used on bending test are cut and used as impact test samples.	Coated surface will be subjected to rapid impact forces to characterize the coating behaviour under sudden impacts.
7.	Electrochemical porosity test	3 of 45, 3 of 90	Coated surface exposed to artificial seawater under the influence of an increased corrosion potential to measure the ability of the coating to keep water from the substrate. This will give knowledge of the amount of pores in the coating.
8.	Erosion	2 of 45, 2 of 90	Coated surfaces will be subjected to a water stream containing erosive particles to characterize the resistance to erosion effects.

## 3.2 Microstructure of coating

The microstructure will strongly influence the coating properties. A high amount of pores in the coating will be detrimental to the corrosion resistance of the coating as water can penetrate to the substrate. It is also important to have an even distribution of hard particles in the softer matrix to prevent excessive wear damages to the weaker parts of the coating, as explained in chapter 2.3.1. Such characteristics can be observed by a microscopical analysis of the cross section of the coating. The coating thickness is able to measure using a length scale provided by the computer connected to the different microscopes used (see below).

A light microscope is a simple method to observe a material surface. A beam of light is directed to the observed surface, which reflects the light to allow us a clear view of the material surface. This type of microscope uses a magnification in the order 50-1000x and can give quick results of the characteristics. The samples observed should be polished to allow adequate light reflection from the surface. For the test samples used for microscopical analysis, a gradual grinding process that included SiC papers were used. The roughness of the papers went through 220, 500, 1000, 2000 and 4000, with a final diamond polishing at 3 $\mu$ m. This provided a mirror like surface for the samples

A Scanning Electron Microscope (SEM) is a more complex way of characterize the material surface and is performed in a separate machine. Two modes on the SEM will be used during the characterization: secondary electron mode to observe details in the surface, and backscatter electron mode. The backscatter mode will light up the elements compared to their atomic weight, thus making it easier to distinguish the different phases of the coating. This microscope allows examination of the samples at high magnification, and gives more detailed and clear observations of the sample.



### 3.3 Hardness test

The hardness properties have a significant influence on the wear resistance of a material. Both adhesive and abrasive wear will decrease as the hardness increases. The mechanism of these types of wear is describes more thoroughly in chapter 2.3.1.

There exist several different tests to determine the hardness on a material, developed to be accurate for different types of materials. Vickers hardness test have been used for these tests. Vickers hardness test utilizes a square pyramid indenter, which is pressed against the material with a known force to make a squared shape mark. The diagonals of the indent are measured with a microscope. The formula for calculating Vickers hardness is found in Equation 1. This formula requires the force (F) in kilograms and average diagonal length (d) left by the indenter.

$$HV = \frac{F}{A} \approx \frac{1,8544 * F}{d^2}$$

**Equation 1: Vickers hardness formula**

The hardness test on the material is done on the cross section surface of the coating. It is important to make sure the indent area do not consist of a mixture of the coating and the substrate material, as the substrate is very soft compared to the coating and will give high deviations in the result.

### 3.4 Roughness

The roughness of a surface is a measurement of the surface texture. There are several different ways of characterizing the roughness of a surface. Roughness is an important factor to determine how the surface will interact with its environment. The most used method in the industry is the measuring of the Ra value. This value is calculated by measuring the average distance between the actual surface and the center line of the profile. The Ra value is based on a lot of experience, but still gives limited information about the actual topography of the surface. All of the profiles shown in Figure 15 have the same Ra value, but will have different behaviour in sliding contact [11].

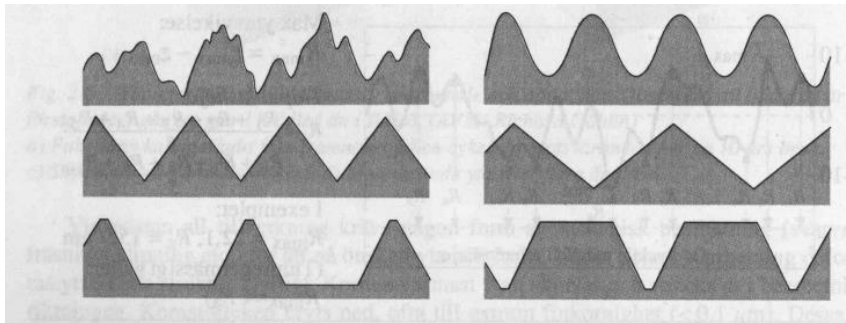


Figure 15: Roughness profiles [11]

To get a better characterization of the profile of the surface, the root mean square value (Rq) can be used [11]. High peaks and low valleys of the surface will affect the calculated value of Rq more than the case for Ra. By calculating Rq, the profiles found in Figure 15 may be differentiated.

The Rz value can also be of interest, as this value gives the average distance between the lowest valley and highest peak in each sampling length.

To calculate the Ra value, the formula shown in Equation 2 is used. Where L is the length measured and the  $z(x)$  value is the peak value on point x, compared to the set center line.

$$Ra = \frac{1}{L} \int_0^L |z(x)| dx$$

Equation 2: Ra formula

To calculate the Rq value, the formula in Equation 3 is used.

$$Rq = \sqrt{\frac{1}{L} \int_0^L z(x)^2 dx}$$

Equation 3: Rq formula

To measure the roughness of the surface, a Mitutoyo SJ-301 profilimeter is used with standard JIS2001 [12]. There is not mentioned any requirements to the roughness of the surface in the test procedure or the demand specification, except for the roughness value to be quantified [13] [1]. However, in the NORSOK M-630 standard there is an acceptance criteria of a maximum value of  $R_a=0,15\mu\text{m}$  [7]. The specification of demand has not made any reference for surface roughness against this standard, but it will still provide a comparison of the results obtained.

### 3.5 Adhesion test

The bonding force between the substrate material and the coating characterizes adhesion of the coating. Testing of this strength is important to control the quality of spraying equipment and procedures.

Standard ASTM C633 proposes a test method to determine the degree of adhesion of a coating to the substrate surface [8]. This test consists of one coated sample, which is glued to an uncoated and sandblasted steel sample using a bonding agent. The bonding agent used is 3M scotch-weld 2214 regular epoxy adhesive. These two samples are to be subjected to a tensile load normal to the plane of coating. By measuring the force needed to pull of the coating, we can determine the weakest part of the system.

The test samples were delivered separately from the bonding agent and the joining of the two test samples had to be done before testing. After the application of bonding agent on the material surface, the two pieces were clamped together to ensure no movement during the curing and that eventual pores in the bonding agent were pressed out. Heating is necessary for the bonding agent to properly cure. The data sheet for the bonding agent proposes three different cycles that will result in full curing [14]:

- 121°C for 40 minutes
- 149°C for 10 minutes
- 177°C for 5 minutes

These time cycles do not take in consideration that the centre of the samples requires longer time to be heated up to the temperatures specified. A test heating of one pair of samples were done before applying the bonding agent to measure the time required to reach a sufficient temperature at the centre of the samples. With the aid of a temperature transmitter connected to the samples, the temperature could be found. At 149°C oven, it took the sample 30 minutes to reach 140°C, and after one hour, the temperature reached 145°C. From this, it was concluded to let the samples cure for one hour at 149°C. Even though the centre does not reach 149°C during this time, they will have stayed above 121°C for a sufficient amount of time.

This test can provide several different results, depending on the location of fracture. The adhesion strength of the coating is given if the rupture is in the coating-substrate interface. The cohesion strength is given if the rupture is within the coating. The ultimate tensile strength of the bonding agent used has to be greater than the required adhesion or cohesion strength of the coating. This means that a rupture through the bonding agent will provide a satisfactory result for the coating, given the force get near the range of ultimate tensile strength. If the failure is from a combination of these locations, the source of rupture can usually not be determined. The standard suggest a microscope with up to 100x magnification to determine the location of failure [8]. A microscopical examination of the cross section of each sample may also be helpful to determine the area of rupture.

This test is done in the workshop of IKT at NTNU. The test samples are fastened to the two adapters from Figure 16. The test samples with adapters from Figure 17 are clamped on the top and bottom of the test setup. The test setup can be seen in Figure 18. When both adapters are properly clamped to the test setup, the test may begin.



Figure 16: Adhesion test adapters

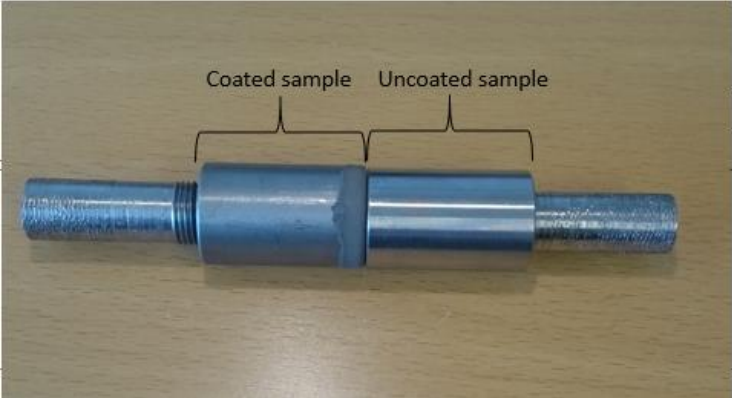


Figure 17: Test samples with adapters



**Figure 18: Adhesion test setup**

Twelve tests have been carried out in total. Five test samples with coating sprayed in a 90 degree angle to the surface, and five test samples with coating sprayed in a 45 degree angle. In addition, two uncoated samples are tested to determine the ultimate tensile strength of the bonding agent, as suggested from standard ASTM C633 [8].

The acceptance criteria are defined in NORSOK-M630 [7]. This part of the standard supplies different acceptance criteria for the material properties for a coating of this type. The minimum bond strength is set to 60MPa.

### 3.6 Bending test

A bending test is used to check the quality of spray parameters and preparation of substrate surface, much like the adhesion test. This test is performed by slowly bending a coated sample to check how the coating behaves. The bending is done in an outward direction, which causes tensile stresses on the coating.

The samples have a dimension of 100x50x2mm and are bent 90 degrees over a mandrel with diameter 25mm. Eight samples are tested in total, which consists of three samples with spray angle 90 degrees and five samples with spray angle 45 degrees. After the test, the sample is visually inspected. From NORSOK M-630, a tungsten carbide coating as used on this test has acceptance criteria of no spalling. Cracking of the coating is expected and acceptable.

The test setup is shown in Figure 19. The test sample (3) are placed on the two supports (1). The mandrel (2) used to bend the plate are to be pushed down. The distance between the supports were measured to about 60mm.

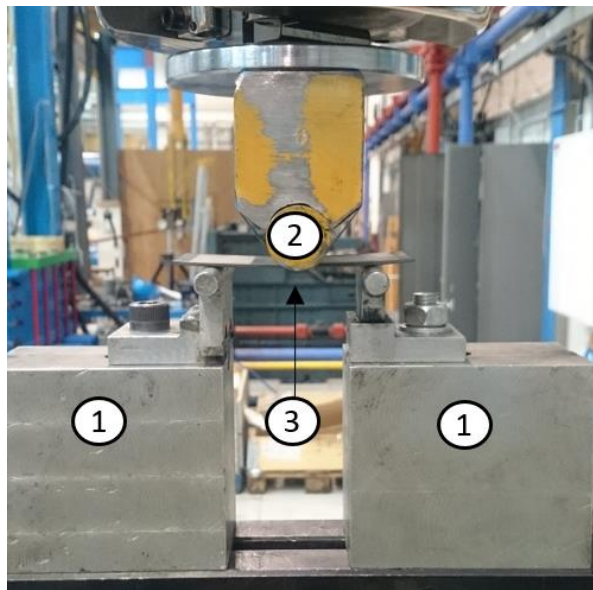


Figure 19: Bending test setup

### 3.7 Impact test

The ceramic coating previously used to protect the piping experienced weaknesses against external forces, as this caused cracking of the coating. The requirements of the coating listed in Table 1 specifies the resulting coating needs to be robust against external forces. To document the properties of the Amperit 560 coating, ISO 6272-1 standard is used [9].

The test proposed in this standard consists of a test rig with a 20mm diameter spherical indenter, which is dropped towards the coated surface with different height and weight additions. The test can be carried out with impacts at the coated side of the panel or the uncoated side, depending on which coating properties that are tested. The standard proposes two ways of testing the coating. Either by a pass/fail test where the test is carried out at a drop height with a specified mass, or as a classification test where the drop height and weight are gradually increased until the coating cracks or peels off. This test will be performed on the coated side of the test panels as a classification test.

The standard suggests making the first drop at a low height with a weight of 1kg, where no cracking is expected. Between each drop, the surface is examined for cracks. If no cracks are visible after inspection, the test will be carried out at an increased height of 25mm. If no cracks are observed after the weight is dropped from the maximum height, an additional kg is added to make the total weight 2kg. The test is afterwards carried out at minimum height, and then increased stepwise as explained earlier. The maximum weight allowed by the standard is 4kg. If cracking is observed at any point, the following procedure is to be done:

The weight is to be dropped on the plate five times at different positions for both the same height as cracking were observed, as well as 25mm below this height, making a total of ten drops. By doing this complete procedure, the weight and height combination that causes cracking, can be determined.

The impact energy can be calculated using the formula in Equation 4, where  $m$  is the mass dropped in kg,  $L$  is the dropped length in meters, and  $g$  is the gravitational constant (9,81  $m/s^2$ ). The calculation will give the amount of Joule at the impact.

$$E = m * L * g$$

**Equation 4: Formula for calculating energy at impact**

As separate test samples were not provided for this test, samples from the bending test had to be used. The undeformed sides of the bending test samples were cut off to give test samples. Four test sample with spray angle 45, and four test samples with spray angle 90 were made. The plate thickness is 2 mm.



### 3.8 Electrochemical porosity test

One reason for coating a surface is to prevent corrosion of the substrate material. The Amperit 560 coating is cathodic compared to the CS, which means the porosity and amount of micro cracks in the coating will be of great significance of how well the surface is protected from corrosion, as explained for non-sacrificial coatings in chapter 2.3.2. A coating with high amount of porosity and cracks, will allow corrosive media to reach the substrate material and initiate corrosion attacks of the less noble metal under the coating.

The corrosion properties of the coating are tested with reference to DNV-C2 [10]. The test is performed by exposing a coated surface to a solution made from distilled water with a 3,5 wt% addition of NaCl. The use of distilled water is to prevent any external contaminations in the water, which could affect the corrosion results. The purpose of this test is to determine how well the coating prevents the seawater to reach the substrate surface. To accelerate corrosion processes that may happen, each of the samples are polarized to -350 mV vs. Ag/AgCl, as specified from the standard. This polarization is cathodic to the coating and anodic to the substrate, which means the substrate will corrode rapidly if the coating allows water to reach through to the substrate. If the coating is successful to prevent any water of reaching the substrate, there will be no corrosion as the coating behaves cathodically under this potential.

The test setup is shown in Figure 20. All the six samples are connected to the potentiostat to be polarized to -350mV vs. Ag/AgCl. Each of the samples are connected to a separate 10 $\Omega$  resistor. To keep the oxygen saturation in the electrolyte, a small pump was connected to the experiment. In addition, it is necessary to connect a reference electrode and a counter electrode to the experiment. Without these, it is not possible to measure any potential or to polarize the samples. By measuring the potential drop over the resistor of each of the samples, it is possible to calculate the current density from Ohms law and thus see how the sample has behaved during the test period.

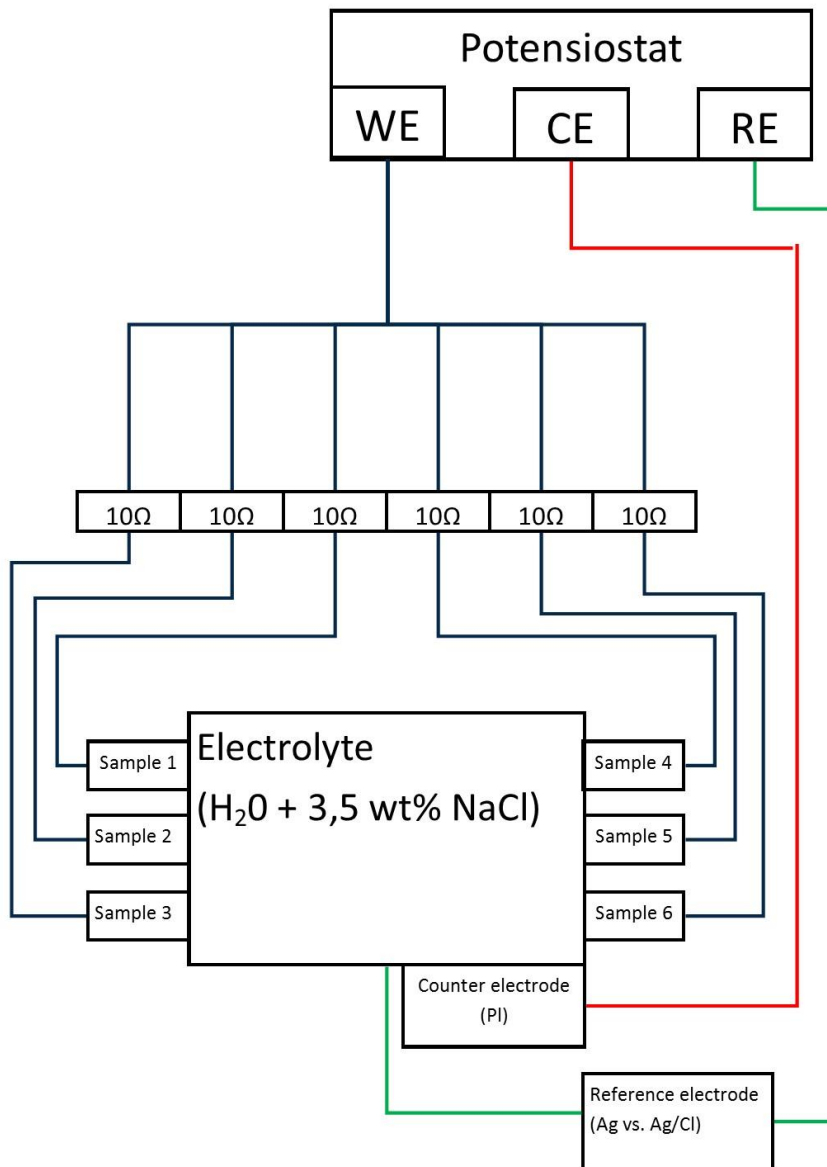


Figure 20: Electrochemical porosity test setup

If the test sample experience corrosion during the test period, there will be a positive potential drop over the resistor. This means water have penetrated the coating and is causing corrosion on the substrate. Depending on the size of the pores or micro cracks, corrosion products plugging the pores may reduce the corrosion attack. If the potential drop measured for the sample is continuously increasing during the test, it means the corrosion is accelerating. A minimum testing time of 500 hours is proposed [10]. This is to check the behaviour of any potential corrosion attacks, if the corrosion is decreased or increased over time. A negative potential value measured means the surface is protected against corrosion attacks.

Corrosion between the substrate and coating will cause reduced adhesion of the coating, as corrosion products will adhere to the coating but not to the substrate. This can cause spalling of the coating, allowing other additional types of attack on the substrate, such as erosion.

### 3.9 Erosion test

As erosion is one of the main concerns of the coating, a test to determine its erosion resistance needs to be performed.

The erosion test rig has been used in a previous master thesis in 2014 [15]. This test used pressurized air to accelerate sand towards the surface. The test rig was modified in a later project study [16]. The air-sand mixer and feeder were changed with an electric motor, which feed sand through a screw feeder. The new test rig uses water instead of air and is shown in Figure 21. The water/sand slurry is fed into a nozzle to accelerate towards the surface. The sample holder is designed to be able to rotate to allow testing of various angles.

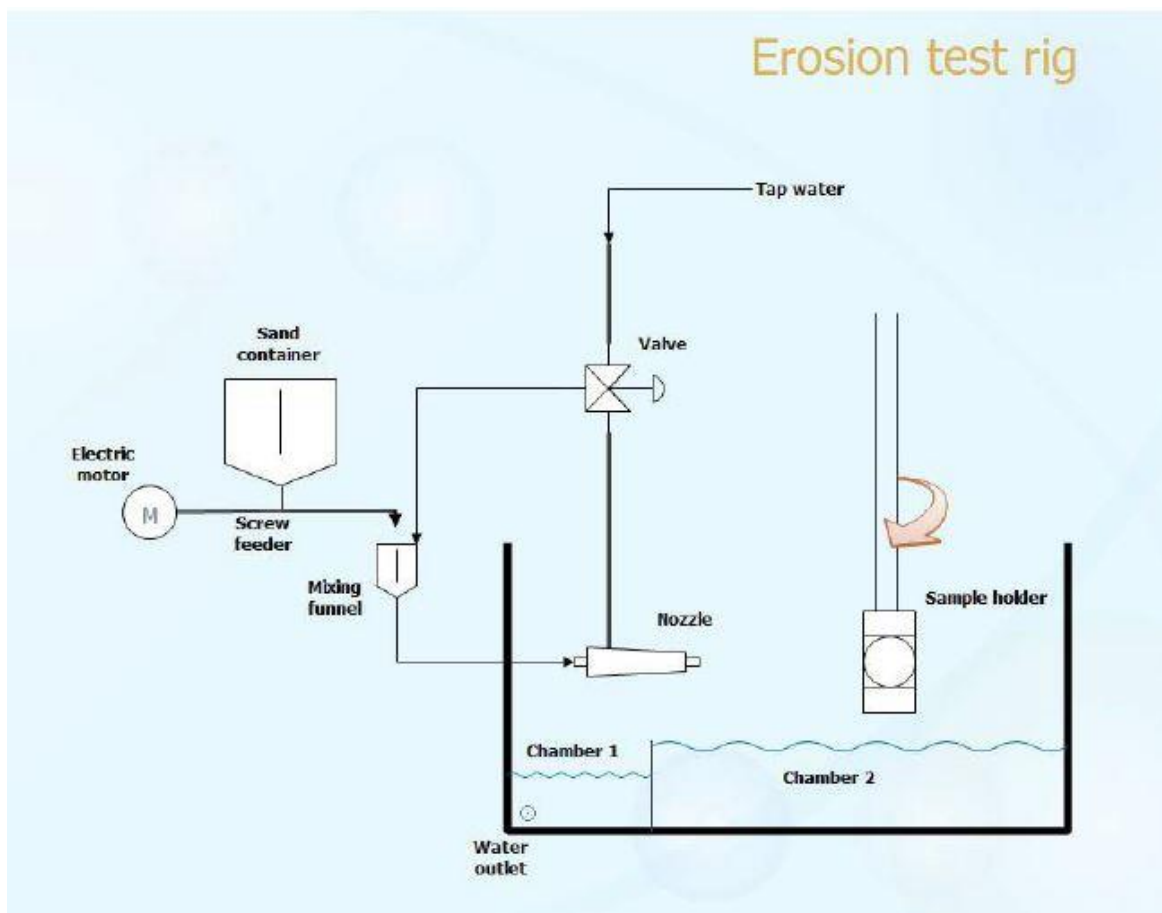


Figure 21: Erosion test setup

The lab test had to be an accelerated test as the real case is under mild conditions. The expected lifetime of the coating is 15 years, and parameters that give test results after a shorter period is required. These proposed accelerated testing parameters are listed in Table 11.

**Table 11: Proposed erosion test parameters**

<b>Parameter</b>	<b>Value</b>
Average particle size in slurry	500 $\mu$ m
Slurry velocity	5 m/s
Particle type	SiC or Al <sub>2</sub> O <sub>3</sub>
Particle concentration	18 wt%
Test angle	45 and 60 degrees

Brown aluminium oxide is used as the abrasive for this test, as this was one of the suggestions from the demand specification [1]. This abrasive was also suggested from the previous work to give a better erosion effect [16]. The grain size used is of type F36, which gives an average particle size of 525 $\mu$ m [17].

## 4 Results

### 4.1 Coating microstructure

The microstructure was observed through a light microscope. The images at x100 magnification is presented in Figure 22 for 45 degree spray angle and Figure 23 for 90 degree spray angle. The images acquired from this microscope were a bit unclear, but it is still possible to distinct the different phases of the coating from their color. From these two figures, the WC-Co phase can be observed by the dark grey spots, while the Ni-Cr-Si phase are the white in between. The CS substrate is observed at the bottom of the pictures. The dark areas in the interface between the coating and substrate are pores.



**Figure 22: Microstructure of 45 degree spray at x100 magnification**



**Figure 23: Microstructure of 90 degree spray at x100 magnification**

The thickness of the microstructure samples were measured to about 350 $\mu$ m, using the scale shown in Figure 24.

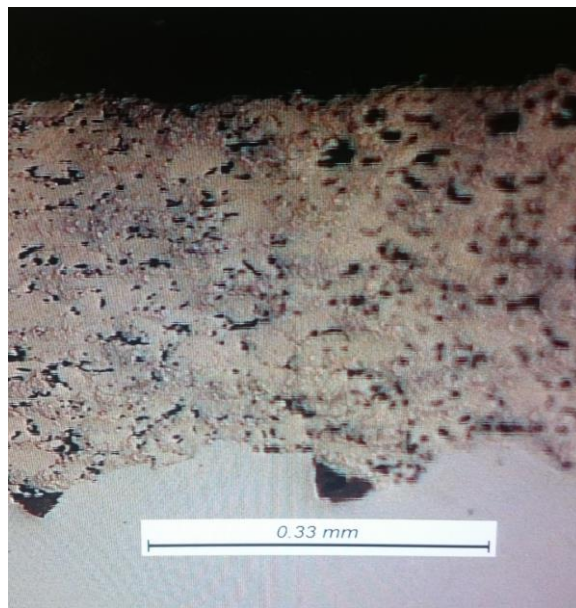


**Figure 24: Thickness measuring**

To get a good view of pores and details at higher magnification, the SEM analysis was used. The color presented in the SEM photos are the opposite from the one from the light microscope, which means the WC-Co phase is white and the Ni-Cr-Si phase is darker, or black.

Figure 25 shows the coating at high magnification. The three main components can be seen in this photo:

- WC is the white grains.
- Co is the light gray phase that surrounds WC.
- The Ni-Cr-Si matrix is the darkest gray matter.

The WC-particles present have a size of 1-2 $\mu$ m.

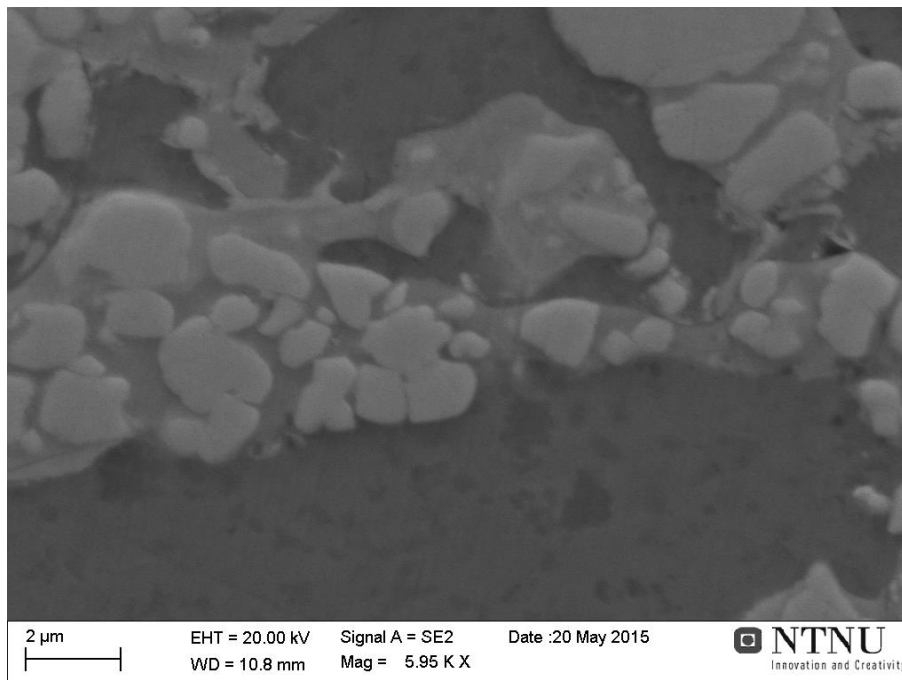


**Figure 25: Different phases at high magnification**



The overview of the two samples in backscatter mode is presented in Figure 26 and Figure 27. Here the different phases can clearly be distinguished. The different angles of spraying clearly gives different microstructure of the coating. The spray angle of 90 degrees, which is displayed in Figure 27, shows a high amount of circular shaped, black spots. This indicates big concentrations of the Ni-Cr-Si phase of the coating that has not been properly melted and deformed during spraying. Figure 26 shows less concentrations like this and the phases are more evenly distributed through the cross section.

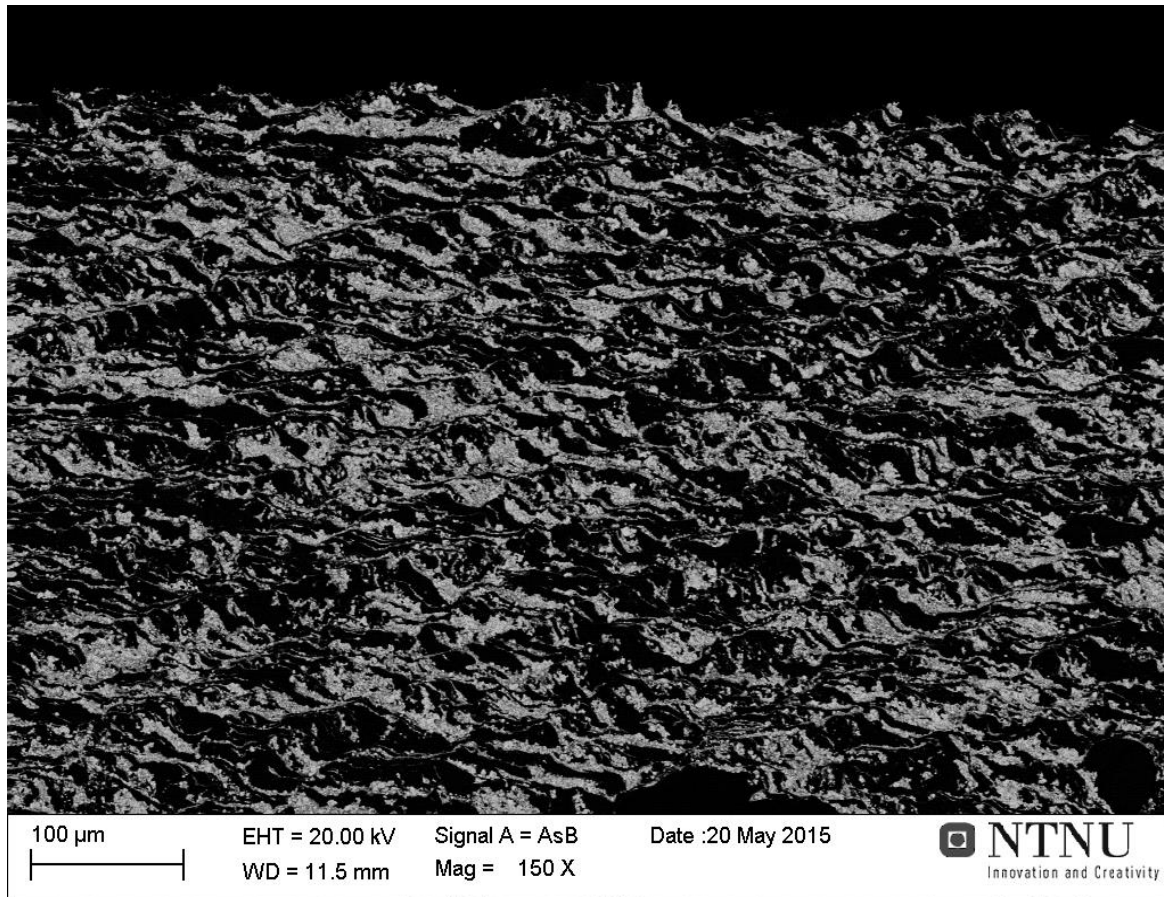


**Figure 26: Microstructure at 150x magnification. 45 degree spray angle**

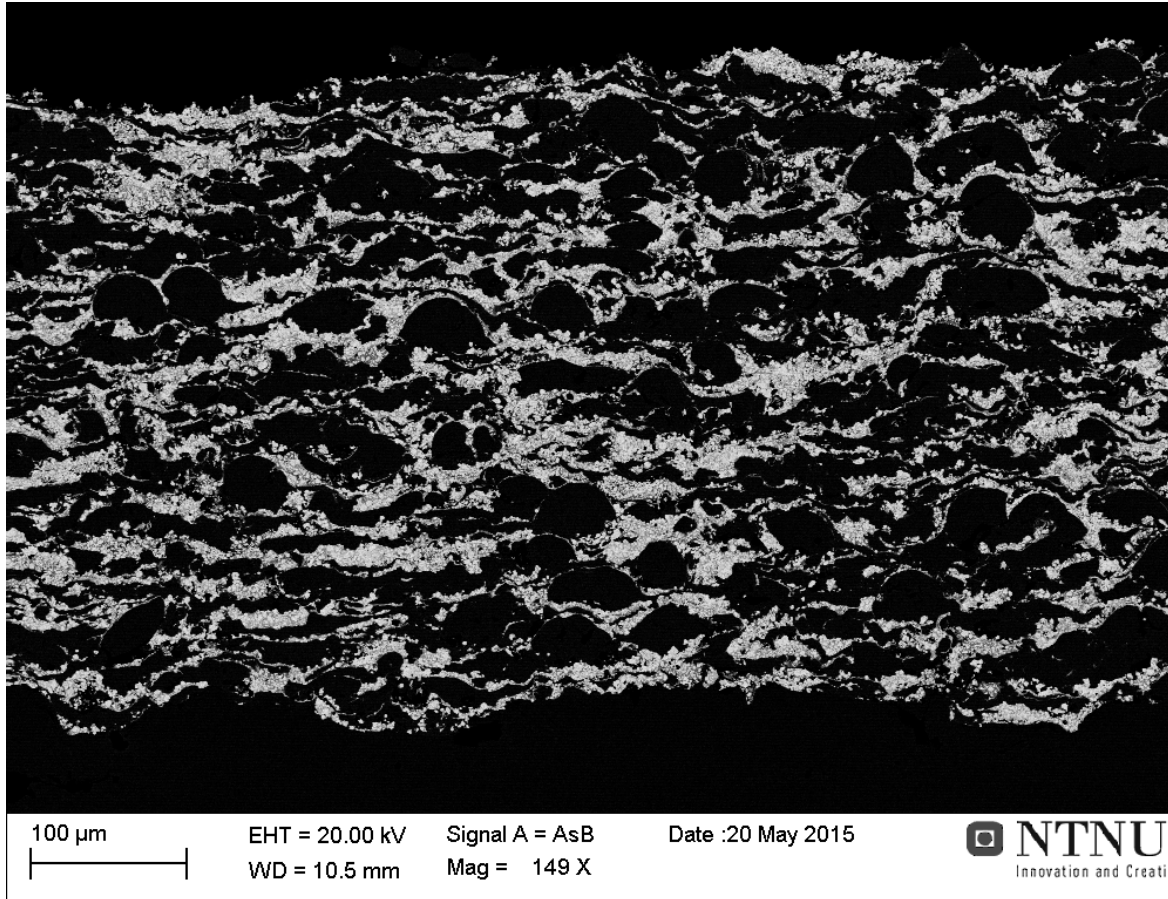


**Figure 27: Microstructure at 149x magnification. 90 degree spray angle**

The red square in Figure 28 shows a pore at high magnification for the coating with 90 degree spray angle. This pore have been formed between the interfaces of two unmelted powder particles. Marked with a red circle Figure 29, there are several areas of unmelted powder particles after one another.

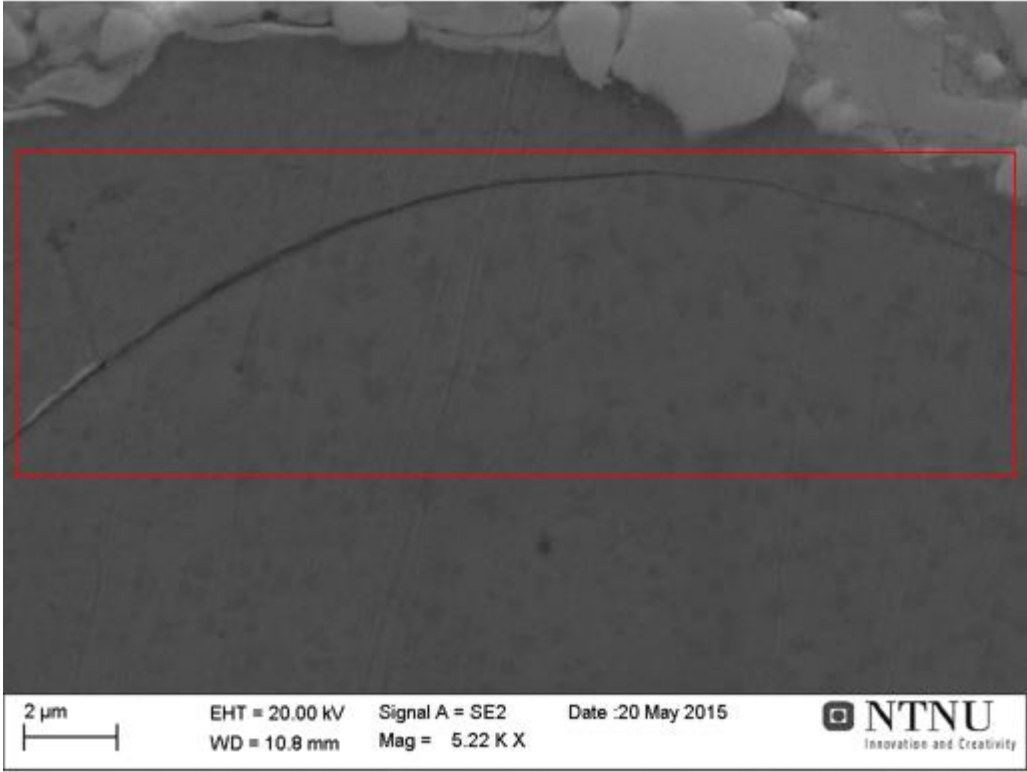
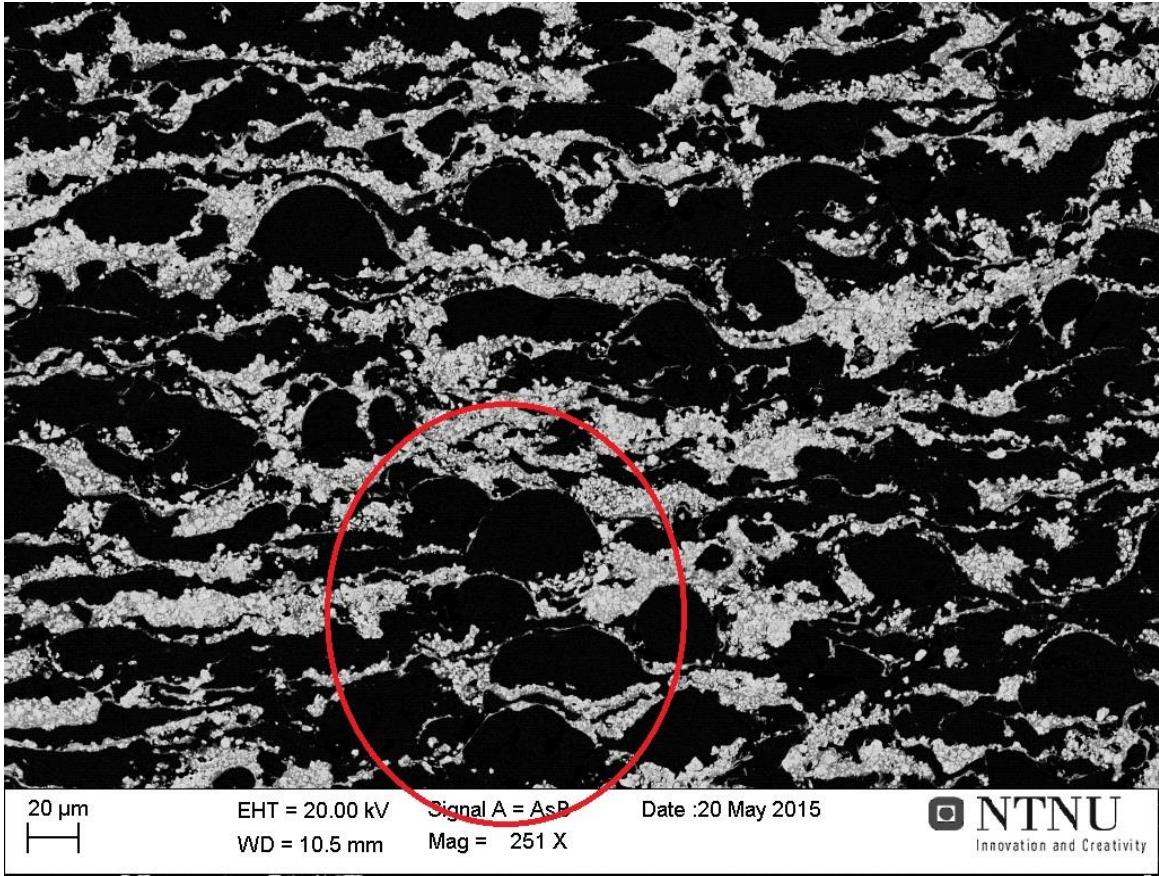


Figure 28: Pore in coating at 5220x magnification



**Figure 29: Unmelted phases through the coating**

Figure 30 shows the coating at 500x magnification, where the phases can be seen as more flat. Few pores were observed on this sample.

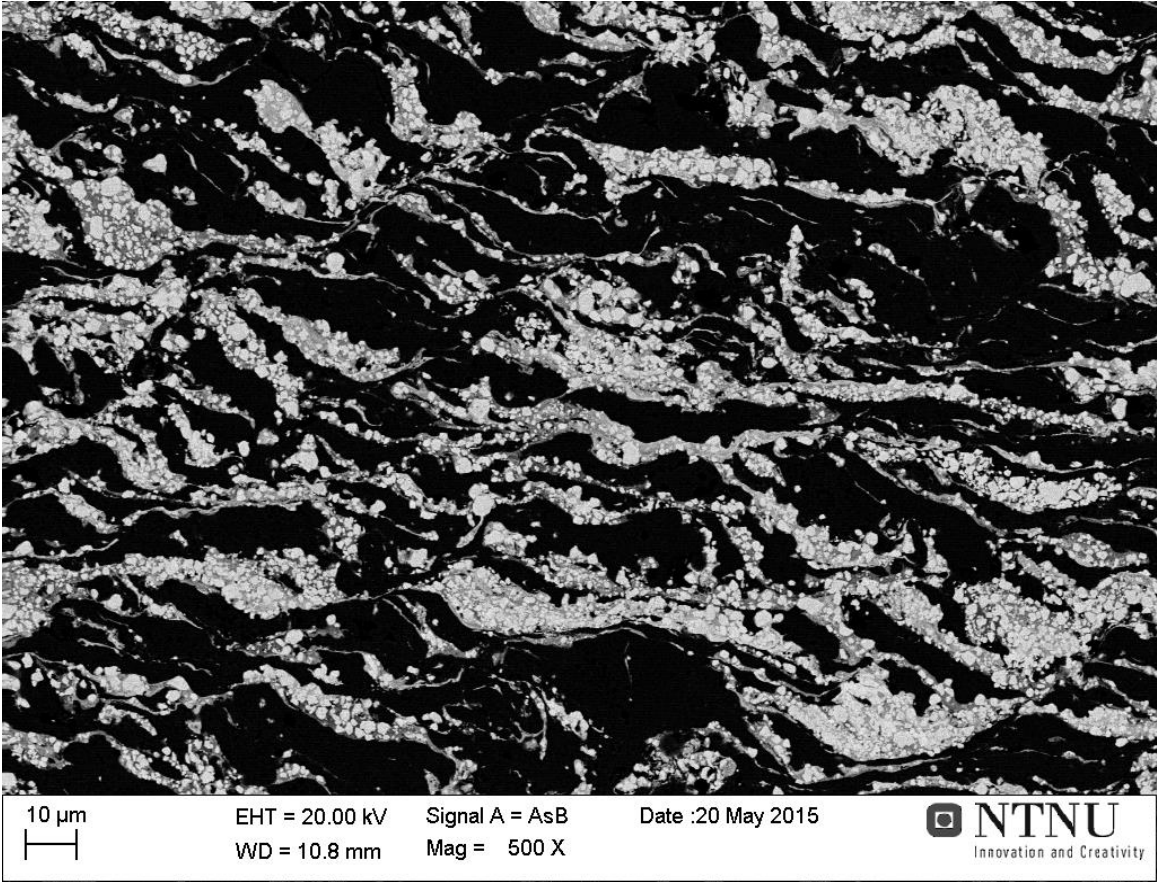
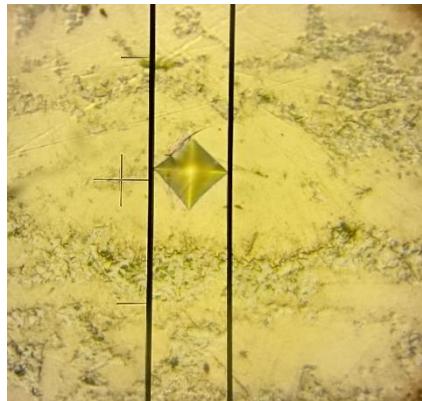


Figure 30: Microstructure of 45 degree sample

## 4.2 Hardness test

Hardness tests were performed on the cross-section of samples with spray angle of 45 and 90 degrees. Hardness measurement for the top surface was attempted as well, but as the surface is rather rough, the indent was hard to measure. Big deviations came from this test, and the values are not taken further into account for this test. The coating tested is a composite coating that consists of different phases which measures hardness values with big deviations. If the indent is taken entirely in the WC-Co phase, the resulting hardness value is very high. Figure 32 shows the indent in the hard WC-Co phase, while Figure 31 shows the measurement from the softer Ni-Cr-Si matrix. These two hardness values were measured to 633HV and 1221HV, which explains the huge difference in the hardness values for this coating. Because of these deviations, a high number of indents should be taken to ensure that a correct average value is measured.



**Figure 31: Soft phase**

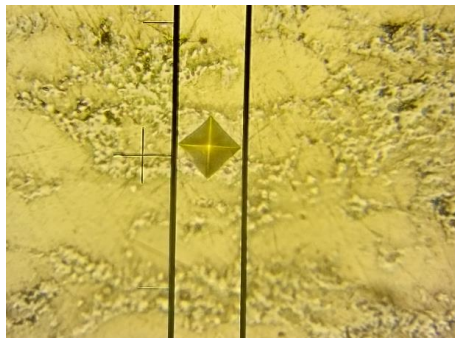


**Figure 32: Hard phase**

The hardness values were taken all over the coating to ensure hardness values both close to the substrate and further away were taken into account. Average hardness values measured for the 45 and 90 degree spray angle is presented in Table 12. All of the measurements and their location are presented in appendix 9.3.

**Table 12: Hardness test measurement**

<b>Sample</b>	<b>Number of indents</b>	<b>Average hardness (HV)</b>	<b>Standard deviation</b>
45 degree sample	32	792	61
90 degree sample	16	839	154

The average hardness values for the two samples do not differ in a huge scale, but the standard deviation has a larger difference.

### 4.3 Roughness

The roughness measurements were taken on a coated plate. The measurements were taken on the surface as delivered without any surface finishing. The test setup is shown in Figure 33.



Figure 33: Surface roughness measuring

Three measurements were done on each sample, with low deviations of the results with each measuring. The measured values in Table 13 are thus representable for the actual surface.

Table 13; Roughness measurements

Roughness	45 degree spray sample	90 degree spray sample
Ra	5,79 $\mu\text{m}$	7,98 $\mu\text{m}$
Rz	37,48 $\mu\text{m}$	47,65 $\mu\text{m}$
Rq	7,16 $\mu\text{m}$	9,76 $\mu\text{m}$

The measured values for Ra are higher than the requirement of 0,15 $\mu\text{m}$  from the standard [7]. However, the standard specifies this value for a surface that is treated to a mirror-like finish. As the surface for this experiment was measured with no treatment after spraying, there is a natural difference in the values.



The test parameters used is listed in Table 14.

**Table 14: Roughness test parameters**

<b>Parameter</b>	<b>Value</b>
Standard	JIS2001
Profile	R
Filter	Gauss
Evaluation length	12,5mm
N	5
$\lambda_c$	2,5mm
$\lambda_s$	8 $\mu$ m
Speed	0,5mm/s

#### 4.4 Adhesion test

The adhesion test samples were fastened to the test setup from Figure 18 and subjected to a tensile load. The tensile load was applied in a constant rate with a cross-head travel velocity of 0,013mm/s, as specified from the standard [8]. The test was carried out until rupture of the sample.

The measured tensile load over time is presented graphically in Figure 34, Figure 35 and Figure 36 where the different sets of samples are separated.

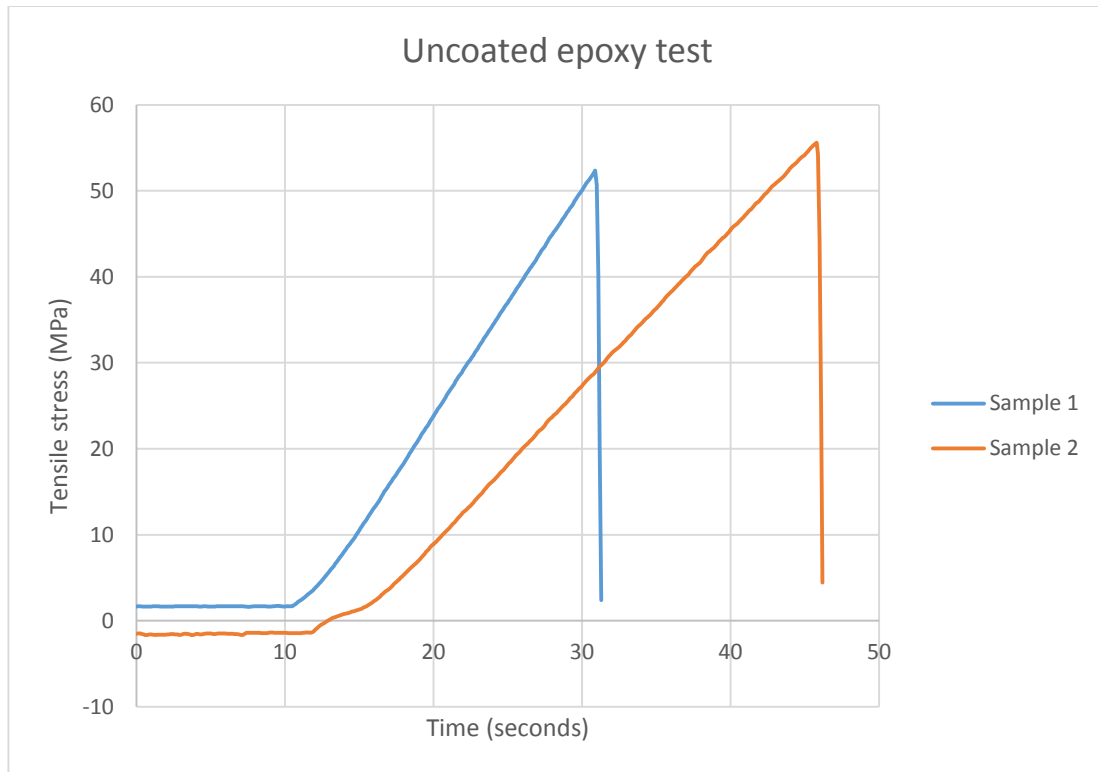


**Figure 34: Adhesion test for uncoated samples**

Sample 1 and 2 from Figure 34 have different slopes due to a change in a cross-head travel velocity. This was done because the first measured value of ultimate tensile stress was below the expected value found in the data sheet, 69MPa [14]. To see if the value went closer to the expected ultimate tensile stress, the velocity was reduced to the lowest value suggested from the standard [8].

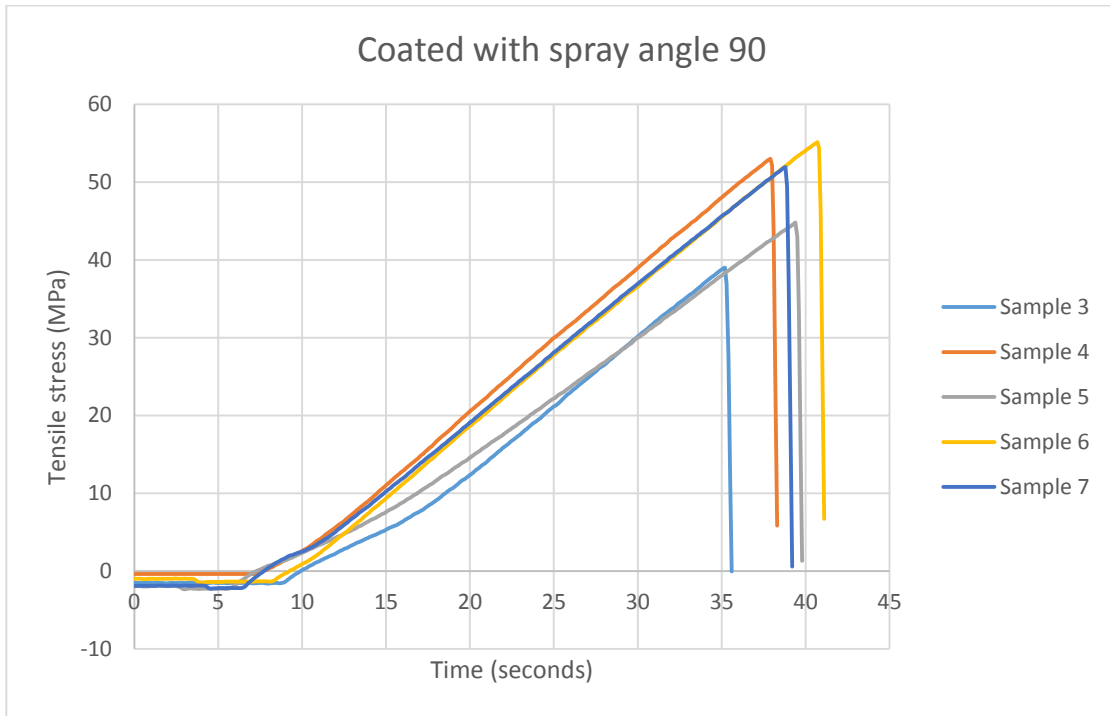


**Figure 35: Adhesion test for samples coated with 90 degree spray angle**

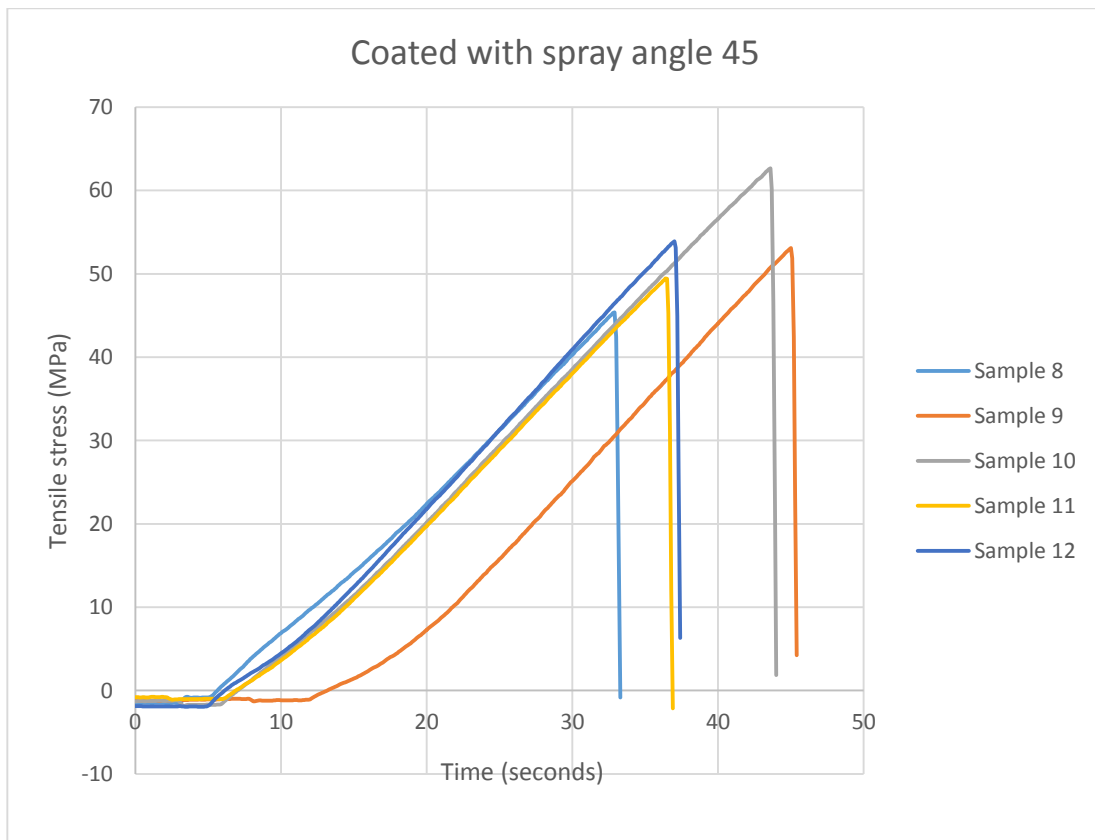


**Figure 36: Adhesion test for samples coated with 45 degree spray angle**

The highest measured tensile strength for each sample is presented in Table 15. The location of rupture is presented as well. The location was determined by examination in light microscope at 50x magnification. These photos are added in appendix 9.5. From this examination, the area of rupture was observed to be in the bonding agent for all samples.

**Table 15: Adhesion test stress and location of rupture**

Sample number	Coating type	Tensile stress at rupture	Location of rupture
1	Uncoated (bonding agent test)	52,36 MPa	Bonding agent
2	Uncoated (bonding agent test)	55,60 MPa	Bonding agent
3	90 degree spray angle	39,03 MPa	Bonding agent
4	90 degree spray angle	53,04 MPa	Bonding agent
5	90 degree spray angle	44,83 MPa	Bonding agent
6	90 degree spray angle	55,17 MPa	Bonding agent
7	90 degree spray angle	51,97 MPa	Bonding agent
8	45 degree spray angle	45,27 MPa	Bonding agent
9	45 degree spray angle	53,11 MPa	Bonding agent
10	45 degree spray angle	62,68 MPa	Bonding agent
11	45 degree spray angle	49,44 MPa	Bonding agent
12	45 degree spray angle	53,92 MPa	Bonding agent

Table 16 presents the average values measured for the three test sets, along with the standard deviation of the measurements.

**Table 16: Average tensile strength at rupture**

Coating type	Average tensile strength at rupture	Standard deviation
Uncoated	53,98 MPa	2,29 MPa
90 degree spray angle	48,81 MPa	6,70 MPa
45 degree spray angle	52,88 MPa	6,46 MPa

#### 4.5 Bending test

Eight test samples were bent as shown in Figure 37. The velocity by the piston was set to 5mm/min, as this had been used with success at an earlier test [16]. The yellow mandrel had a diameter of 25mm and the distance between the supports were 60mm.



**Figure 37: Bending test**

After the test samples were bent 90 degrees, they were removed from the test setup and visually inspected for cracks and spalling of coating. The result from sample 1 is shown in Figure 38. The cracks in the coating are clearly visible over the deformed area of the plate. This behaviour is expected when bent 90 degrees. All of the eight test samples experienced cracking of this type, and the cracking pattern was similar for all samples. No coating spalling was observed for any of the samples, which qualify the coating with regards to the standard used [7].

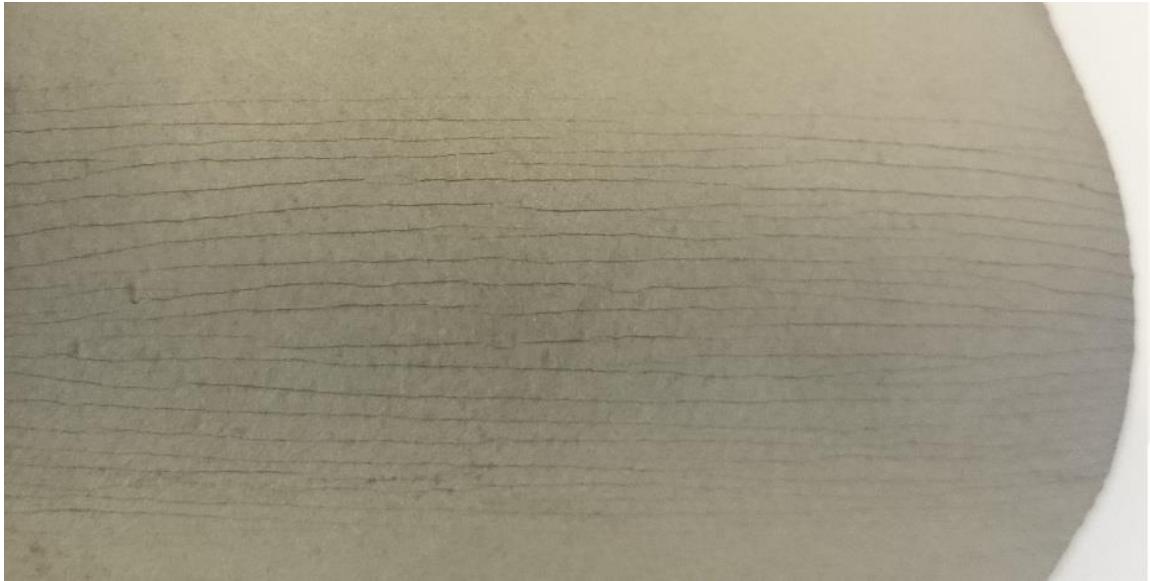


**Figure 38: Sample 1 bending test**

All of the test samples from both the 45 and 90 degree spray angle gave the same results regarding crack pattern and no spalling thus meaning sample 1 from Figure 38 is representative for all of the test samples. Photos of the other seven test samples are included in appendix 9.4.

The applied force vs. time of the pushing piston for all seven samples is presented in Figure 39. Elastic deformation of the plates can be seen in the first slope of the graph, up to about 0,7kN of force. From here, a plastic deformation is observed. This is normal behaviour of steel under deformation. Small movements in the supports in the test setup can explain the large deviations happening around 150-200 seconds. During the initial pressure on the test sample, the sides of the test support got tilted by a few mm, which is seen at the left picture in Figure 40. After the plate had been bent sufficiently, the force downwards on the supports was reduced, and the support fell back into place, as seen on the right in Figure 40. This caused some relief in the applied force, which shows in the graph in Figure 39. As this did not cause any unexpected results on the test samples, the testing continued with the same test setup. The behaviour after 200 seconds can be explained by a small gradual slipping of the test sample at high bending angles.

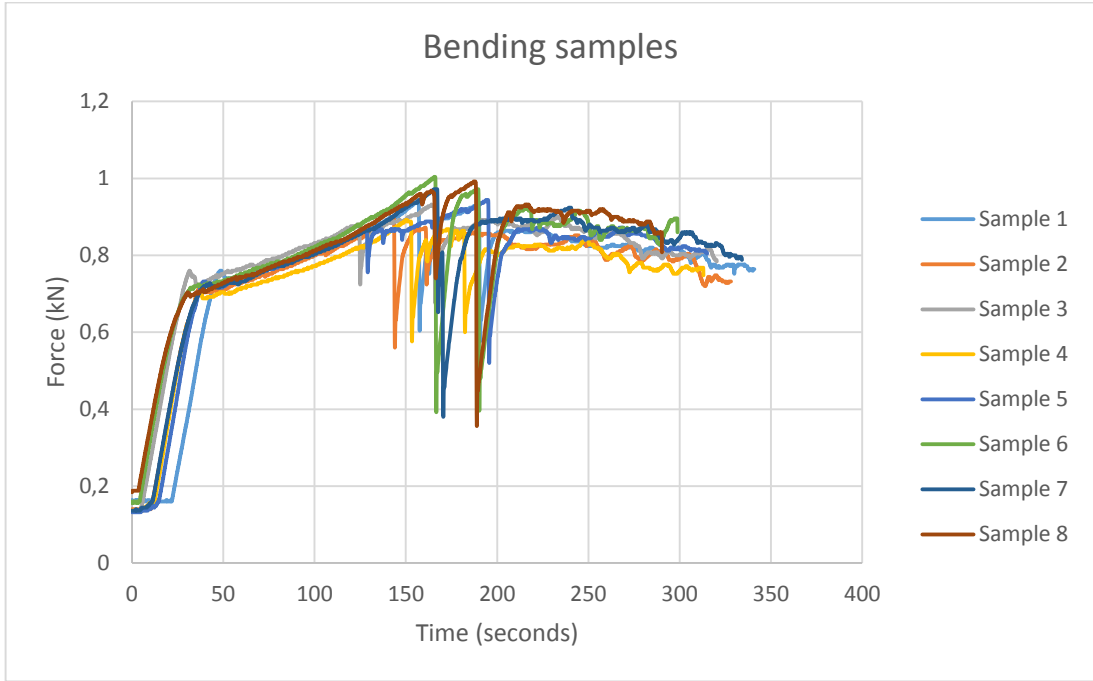


Figure 39: Force applied on bending samples



Figure 40: Support movement during bending test

## 4.6 Impact test

As separate test samples were not provided for this test, samples from the bending test had to be used. The undeformed sides of the bending test samples were cut off to give test samples. Four test samples with spray angle 45, and four test samples with spray angle 90 were made.

For the first test sample, the weight was set to 2kg and 50cm drop distance. This resulted in a large deformation of the test sample at the impact zone with the size of 5mm. Cracks could be observed around the deformed area, along with some spalling of the coating. This is circled red in Figure 41.



Figure 41: Cracks and spalling of sample 1

The weight was reduced to 1kg at a height of 30cm, and the test were initiated once more. This gave deformations at the sample, but not cracking. The height was gradually increased with no sign of cracks, however for a height of 50 cm cracking were observed. Cracks were observed for the other samples of 45 degree spray angle.

The samples with spray angle 90 showed better results for this test as the cracking initiated at higher energy values. As the test samples were rather small, the amount of testing possible on one sample were limited. The gradual increase in height occupied most of the available area at the samples, and this caused bad quantitative results for this test. Cracks for the 90 degree spray samples were observed with a weight of 2kg at 40 cm height, but this only applied for two samples. The two remaining samples had too many impacts to be used further.

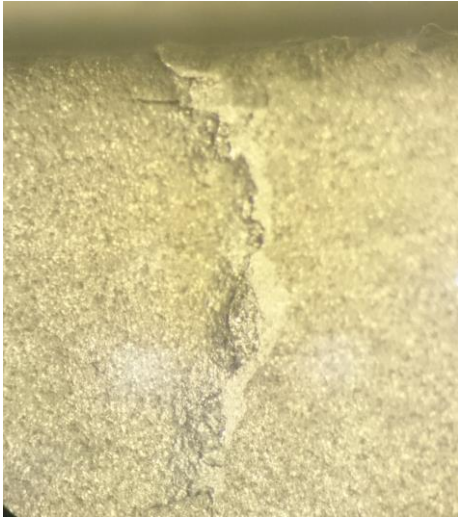
From this test, the values from Table 17 can be obtained.

Table 17: Impact energy values

Sample	Height dropped	Weight	Impact energy
45 degree spray	0,5m	1kg	4,91 J
90 degree spray	0,4	2kg	7,85 J



Some of the tests attempted were taken too close to the edge of the sample. This caused a longer area of deformation, which went from the impact area all the way to the edge. This resulted in a high amount of cracking along this pattern, as shown in Figure 42.



**Figure 42: Cracks near edge of impact test**

The cracking observed for the samples were mostly in the transition area between deformed and undeformed material. The cracking pattern is shown in Figure 43. This pattern followed the circular shape of the impact area.



**Figure 43: Cracking pattern for impact test**

## 4.7 Electrochemical porosity test

### 4.7.1 OCP measurement

At first, the six test samples were not connected to the potentiostat. They were only connected to the reference electrode to measure the Open Circuit Potential (OCP). This was done for 24 hours to let the OCP stabilize. The measured values for each of the samples are listed in Table 18. From these measurements, all of the samples except sample 5 should show a positive current when polarizing to -350mV vs. Ag/AgCl as these have an OCP more negative than the polarisation value.

**Table 18: OCP measurement after 24 hours**

<b>Test sample</b>	<b>Spray angle</b>	<b>Measured OCP [mV vs. Ag/AgCl]</b>
1	90	-368
2	90	-399
3	90	-388
4	45	-388
5	45	-343
6	45	-381

#### 4.7.2 Current density measurement

The polarisation were started. As long as the test was ongoing, the potential drop over the resistor was measured. The values logged during the test was plotted into an excel spreadsheet to make a graphical presentation of the development of corrosion current density over time. The development of the corrosion current density for samples 1, 2 and 3 with a spray angle of 90 degrees, are plotted in Figure 44, while samples 4, 5 and 6 with a spray angle of 45 degrees are plotted in Figure 45.

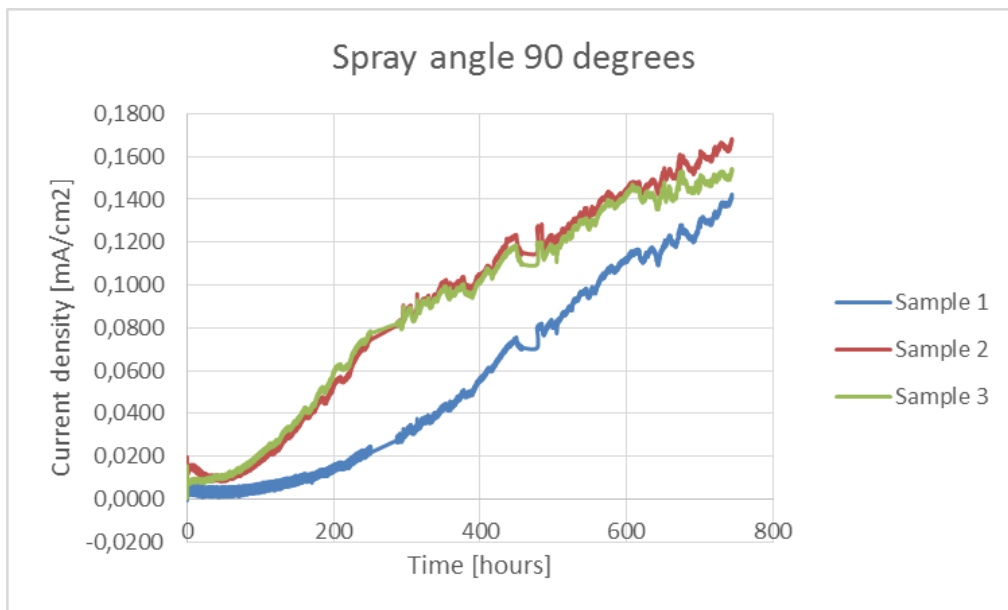


Figure 44: Current density 90 degrees

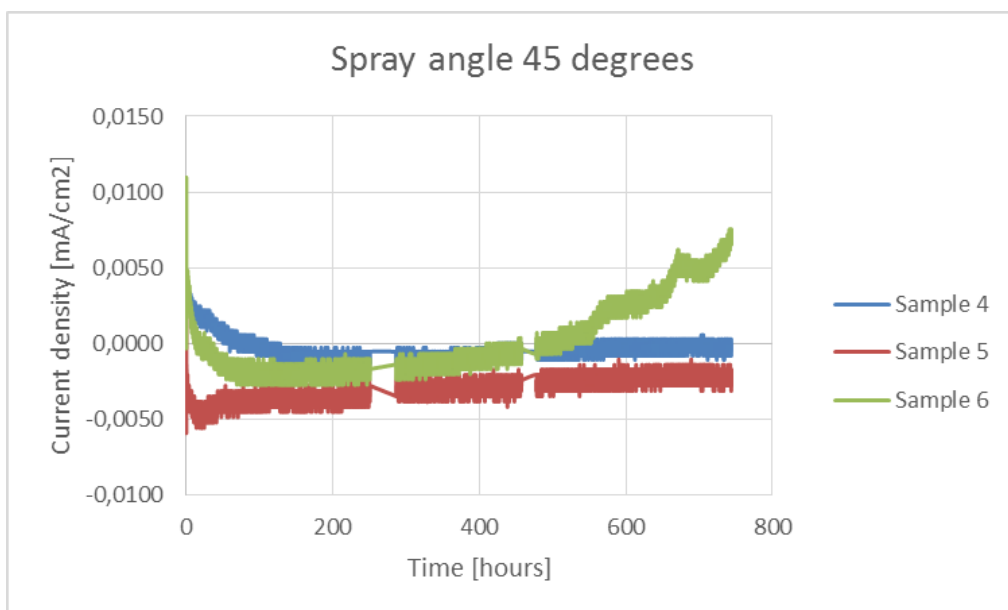


Figure 45: Current density 45 degrees

There is a significant difference in the measured values for corrosion current density between the two sets of samples. It is important to notice the values on both of the y-scales as they scale differently.

Figure 44 shows an almost immediate acceleration of the corrosion rate. Even though the first 50 hours shows a current measurement close to zero, the rate from here on increases over time. Throughout the test length, the corrosion rate kept increasing, with few or no periods that could indicate a reduction or stagnation of corrosion rate.

Figure 45 shows a relatively stable development of the corrosion current density over time, with measured values close to zero. Compared to the first hours of testing, the corrosion rates for sample 4 and 6 experienced a slight reduction until the 100<sup>th</sup> hour, where the rate stabilized. Sample 4 and 5 experienced slightly negative values during the test, which indicate a cathodic behaviour. After about 500 hours of testing, sample 6 experienced an increase in the corrosion rate compared to the two other samples, and this kept slightly increasing during the rest of the test period.

### 4.7.3 Visual inspection

The samples were polarized for 1 month without any change of electrolyte or stops in the polarization. A picture of the test beaker after one month is shown in Figure 46. As seen here, the electrolyte has gained a significant brown color. In addition, considerable amounts of corrosion products are observed on the bottom of the test beaker. From these observations, it shows corrosion on one or more of the samples during the test.



**Figure 46: Corrosion test after one month**

The samples were removed from the beaker, and observed without any cleaning. Figure 47 shows all of the six samples. Sample 1, 2 and 3 shows a difference compared to sample 4, 5 and 6 with a darker brown color on the exposed surface.

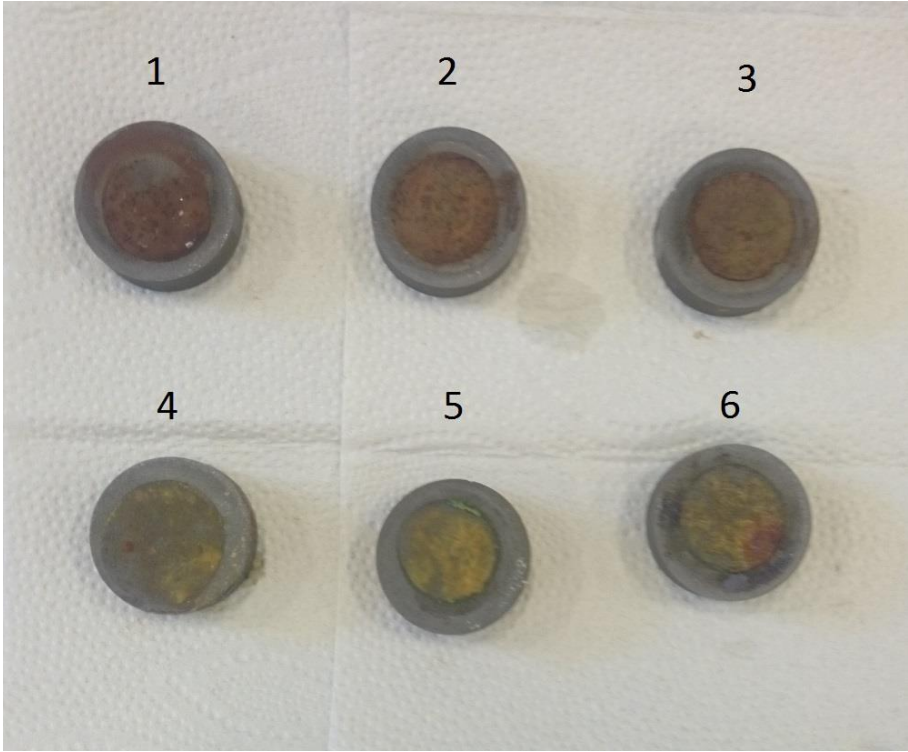


**Figure 47: Corrosion test samples after test completion**

The two sample sets were cut to observe the cross section of the coating. The cross section of sample 1,2 and 3 are shown in Figure 48. The coating can be seen on the top part on the samples. For these three samples, the coating has lost its adhesion to the substrate under the exposed area.



**Figure 48: From left to right: sample 1, 2 and 3**

The coating could be peeled off by hand to expose the substrate, as shown in Figure 49. A corroded carbon steel surface could be seen under the coating. As sample 2 and 3 show the same results for the cross section, this would be the case for them as well.

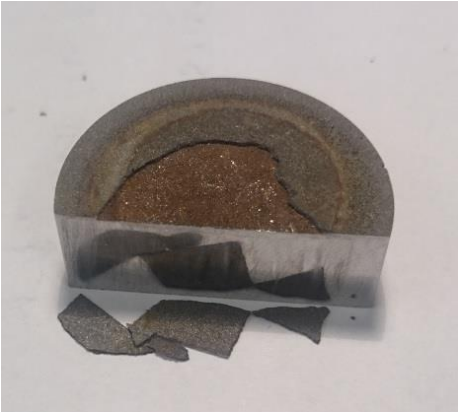


**Figure 49: Peeled surface of sample 2 corrosion test**

Sample 1 was observed in a light microscope. Figure 50 and Figure 51 are from the corroded area of the cross section. The adhesion loss between the substrate in the coating is visible. In addition, Figure 50 shows some amount of degradation of the coating.

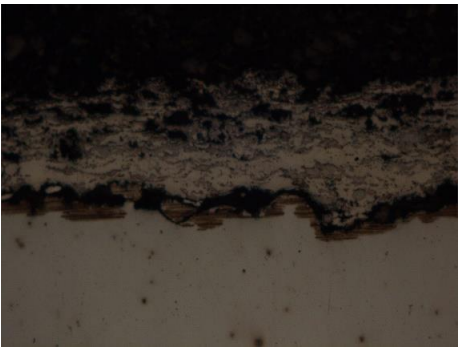
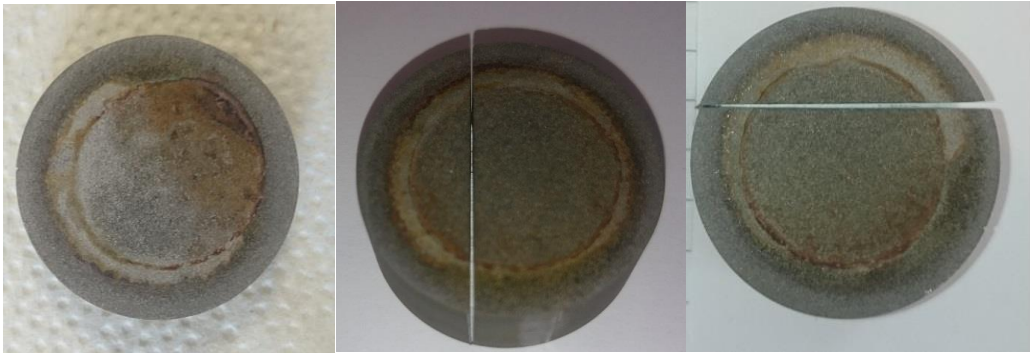


**Figure 50: Sample 1 cross-section at 50x magnification, degraded coating**



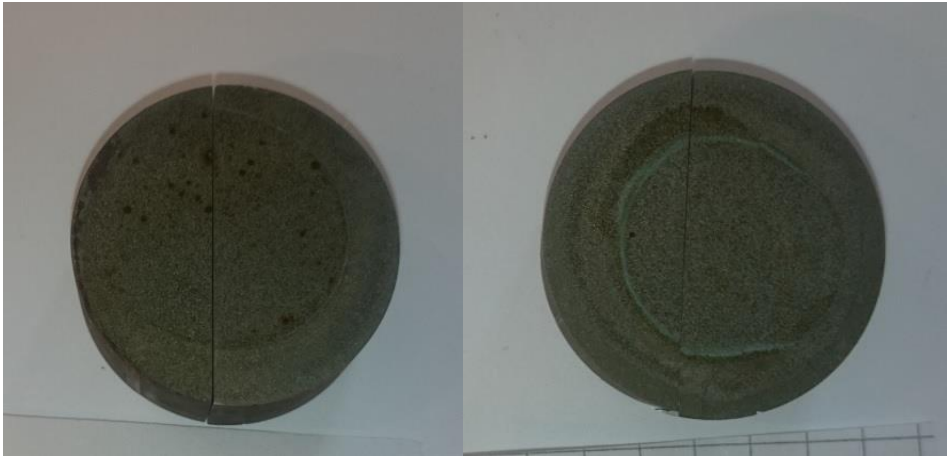
**Figure 51: Sample 1 cross-section at 50x magnification, adhesion loss**

Figure 52 shows the coating surface of sample 1, 2 and 3.



**Figure 52: From left to right: Sample 1,2 and 3 corrosion test**

The visual inspection of sample 4, 5 and 6 provided different results. No delamination of the coating on sample 4 or 5 were observed. Sample 6 showed some local delamination, but over a smaller area than for sample 1, 2 and 3. The surface of sample 4 and 5 are shown in Figure 53. The surface of sample 4 to the left shows some small areas of corrosion, while sample 5 to the right is mostly free of such spots.



**Figure 53: From left to right: Sample 4 and 5 corrosion test**



The complete surface area for sample 6 along with the spot of delamination is shown in Figure 54. On the right picture, the delamination is circled. The area of delamination is under the circled surface of the left picture. This shows a browner surface compared to sample 4 and 5. In addition, crevice corrosion that has occurred under the gasket is visible on the lower part of the sample. This area was supposed to be masked from exposure to the electrolyte, but water has gotten between the gasket and the coating to cause a corrosion attack. The delamination is under the exposed area of the sample, not directly under the crevice.



**Figure 54: Sample 6 corrosion test**

#### 4.8 Erosion test

The actual erosion jet parameters for this project are calculated as follows:

Water flow rate:  $Q = 3,55 * 10^{-4} \text{ m}^3/\text{s} = 21,3 \text{ l}/\text{min} = 0,355\text{l}/\text{s}$

Nozzle dimension:  $d = 9,53\text{mm} \rightarrow A = 71,14\text{mm}^2 = 7,11 * 10^{-5}\text{m}^2$

Water velocity:  $v = \frac{Q[\frac{\text{m}^3}{\text{s}}]}{A[\text{m}^2]} = \frac{3,55 * 10^{-4}}{7,11 * 10^{-5}} = 4,99 \text{ m}/\text{s}$

Water mass rate:  $m1 = 355 \text{ g}/\text{s}$

Sand mass rate:  $m2 = 10,2 \text{ g}/\text{s}$

Weight percentage sand in slurry:  $\text{Sand wt}\% = \frac{m2}{m1+m2} = \frac{10,2}{355+10,2} * 100\% = 2,8\text{wt}\%$

The samples tested and the parameters used, are listed in Table 19. The same amount of sand were used for all samples.

**Table 19: Test parameters for erosion test**

Sample	Coating spray angle	Erosion jet angle	Amount of sand used
1	45	45	100kg
2	45	60	100kg
3	90	45	100kg
4	90	60	N/A*

**\*Test had to be aborted due to breakdown of sand feed motor**

The visual result of sample 1, 2 and 3 are presented in Figure 55, Figure 56 and Figure 57. The area exposed to the erosion jet is visible as the blank area in the centre of the samples. Sample 1 have a dimension of 50x100mm, while sample 2 and 3 have a dimension of 50x120mm. The main area of exposure were measured to a diameter of 25mm.



**Figure 55: Sample 1 after erosion test**



**Figure 56: Sample 2 after erosion test**



Figure 57: Sample 3 after erosion test

The results from the erosion test is presented in Table 20. A weight measurement were done before and after test to check for deviations. A roughness measurement were done after the test on both inside and outside the exposed erosion area.

Table 20: Test results for erosion test

Sample	Weight before	Weight after	Roughness outside exposed area		Roughness inside exposed area	
			Ra	Rz	Ra	Rz
1	411g	411g	4,06 $\mu$ m	23,07 $\mu$ m	1,02 $\mu$ m	5,47 $\mu$ m
2	477g	477g	3,86 $\mu$ m	21,43 $\mu$ m	1,2 $\mu$ m	6,28 $\mu$ m
3	477g	477g	4,62 $\mu$ m	26,22 $\mu$ m	1,4 $\mu$ m	7,38 $\mu$ m
4	413	N/A	N/A	N/A	N/A	N/A

## 5 Discussion

### 5.1 Microstructure

The microstructure of the samples deviates with the spray angle used. Except for the corrosion test and small hardness variations, there were not any significant differences in the rest of the tests between test samples with 45 and 90 degree spray angle.

The pores formed between the substrate and coating are large. They are most likely formed due to the roughness of the sandblasted carbon steel surface. Roughness peaks on the substrate may provide a shade where the coating do not reach. However, some of these pores seem to be in rather flat areas. This can indicate large air pockets present during the initial spraying on the substrate surface. Some of the smaller pores observed are due to carbides and material being torn off during the sample preparation process, but the large pores are unlikely to have formed because of this.

The supplied data sheet do not supply any information regarding the size of the WC particles, and do not give the possibility of comparing the actual sizes to expected values. The data sheet just supplies the size of feedstock powder used.

A high amount of unmelted areas through the coating gives room for pores to be established. The pore gaps found in the sample sprayed 90 degrees are not very big, but it could still provide a way for corrosive media through the coating.

Unmelted phases described earlier could not be found in such a large scale on the microstructure for the coating with 45 degree spray angle. This indicates a higher amount of deformation of the spray powder.

### 5.2 Hardness

The 90 degree spray samples proved to have large areas of unmelted material. As this surface seems to be less blended compared to the 45 degree spray, this could explain the increased standard deviation of the hardness measurement.

Different forces were used for the two samples. Even though the formula takes into account an increased force to give a larger indent area, the hardness values may differ. On an Amperit 560 coating, there are different phases throughout the coating, giving different hardness values. While the 45 degree sample had an indent load of 2000 grams, the 90 degree sample only had 300 grams. This means the indent will reach deeper for the 45 degree sample and measure for a larger area. A larger indent area will reduce the probability of measurements in pure phases of WC-Co or Ni-Cr-Si, which gives deviations in the results.

The acceptance criteria from the NORSOK M-630 standard is set to be 1000HV in average. The measured values found in this test deviates from this acceptance criterion. However, as explained earlier, this coating consists of 50/50 WC-Co and Ni-Cr-Si, which means it will experience a lower hardness compared to a standard WC-Co. The measured value in the WC-Co phase was found to be 1221, which is above the value specified in the standard.

### 5.3 Roughness

The surface of the coating was not treated in the way the standard suggests [7]. Because of this, a high roughness of the coating was measured. A treatment to make a mirror like surface like proposed in the standard will have to be done to achieve the surface roughness recommended.

There surface sprayed with a 90 degree angle showed a slightly higher roughness compared to the sample sprayed 45 degrees.

### 5.4 Adhesion

The adhesion test showed promising results as none of the rupture areas went through the coating, but at the bonding agent. The downside for this test was the low values measured. From the data sheet, the bonding agent was supposed to have an ultimate tensile strength of 69MPa, but none of the test came as high as this. A possible explanation for the results can come from the test setup. All of the separate parts used in the setup were rigid, without any possibilities to compensate for eventual misalignments in the bonded test samples. This means the possibilities of shear stresses through the test samples are present. A shear stress in addition to the tensile stress of the test can cause forces between the test samples to make the rupture occur at an earlier point, and thus explain the values measured for this test. A test setup with bearings designed to compensate for misalignment, and direct all force normal to the test surface could prove to give different results.

Introduction of bubbles in the bonding agent during application is a possibility. Even though a clamp was used to apply pressure to the samples after application of the bonding agent, there are no securities against pores present.

A poorly cleaned surface will experience a loss of adhesion, as the bonding agent adheres to the dirt instead of the surface. In this case, all of the surfaces were cleaned with ethanol and put in an ultrasonic bath before applying the bonding agent. The probability of reduced adhesion due to dirt is consequently low.

The samples sprayed with a 90 degree spray did not show any weakness in adhesion or cohesion strength compared to the samples sprayed 45 degrees. A high amount of pores and unmelted material in the coating could compromise the cohesion strength, but this was not found in this test. A higher strength bonding agent could show to provide results, which separates the two spray parameters

The requirement of the coating was to have an adhesion strength of min. 60MPa. Only one test experienced this force, and the coating was still intact after the rupture. Even though the rest of the coating tests did not experience the required strength, they may still be acceptable and supply the required adhesion strength. The forces measured are the minimum values that the coating can withstand, and may as well be greatly higher and in the acceptable zone.

## 5.5 Bending

The movements in the supports during the bending test caused a small relief of the pressure on the plates. This means the bending force was not constant though the test. Even though this happened, the results obtained were satisfactory. The force required to bend the plates are not of great significance for this test, and the visual inspections after bending are the only method of qualifying the coating. As the plates got bent 90 degrees, this test was successful. The test showed cracking as expected, but the coating adhered to the surface without spalling.

## 5.6 Impact

The plates used for the impact test proved to be weak against deformation. The coating seems to have suffered due to this as the cracking is mostly in the deformed area. A test using thicker plates would most likely not experience the same cracking of the coating as observed here.

Some test areas were done close to the plate edge. This caused visible cracks from the area of impact to the edge. Plates made for this test with a larger test area would be beneficial as the impact could be done further from the edge, and with more space between each impact.

The fact that the impact would have to be taken close to each other seemed to affect the coating cracks. Two impacts close to one another will provide opposite tension effects in the coating, and give more stresses on the coating surface. This seemed to be the case as cracking not previously present in an area, occurred after impact number two. The values found from this test have too many sources of error and are not in high enough quantity to give any conclusion.

Even though the plate deformation may have affected the results of the coating, some results can still be obtained from the test. As the samples experienced cracking in the coating, it shows how brittle the coating is. The previously used ceramic coating proved to be weak against external forces, and could crack when the pipes are exposed to impacts during transportation and handling. For pipes with a thin wall thickness, the Amperit 560 coating used in this test could also be susceptible to external local forces. The parameters of 1kg mass released from 50cm caused cracking for most of the test samples. This amount of energy is not very high, and can be experienced on the pipes during transportation and assembly.

## 5.7 Corrosion

The OCP values will vary depending on the quality of the coating. The coating will supply one OCP value and the substrate another. The two phases will push the measured OCP value in opposite directions depending on the amount of exposure to the electrolyte. Values of OCP can be characterized as a mix-potential between the two phases. If more water is allowed to reach the substrate surface, the OCP will be pushed in the direction of the substrate. The opposite will be experienced if pores are plugged to reduce the substrate surface exposed.

There is a huge difference in the corrosion test between the two spray parameters. Both the measured values and the visual inspection showed poor corrosion resistance of coating sprayed with 90 degree angle. The coating has spalled all over the exposed area for all samples. The coating microstructure observed for this spray parameter presents a high amount of unmelted phases through the coating with the presence of pores between them. This seems to have a huge effect on the amount of water penetrating the coating, as the sample set with 45 degree spray angle experienced almost no corrosion in comparison. The spray angle of 90 degrees are usually the best angle in standard conditions, but show worse results for this coating. The high amount of unmelted phases and pores in the 90 degree coating may be due to poor spraying parameters. If the particles spend a low amount of time in the spray flame, it will cause a lower amount of heat input to the particles, making them less molten. A spray angle of 45 degrees enables an increase of spraying distance, causing the spray particles to stay in the spray flame for a longer time. This can be an explanation to the higher amount of melted phases for the 45 degree coating.

For one test sample, the area under the gasket showed severe crevice corrosion. This can prove a weakness in the coating against this corrosion type. As only one sample showed this, not enough data is present to quantify these results. The other gaskets used may have proved better to keep the water from penetrating the surface, and thus not causing any crevice corrosion. The area of spalling in sample 6 is close to where the crevice corrosion has initiated. This may indicate this have started a corrosion process, and allowed water to penetrate the coating under the crevice, to reach the substrate. From the graphical data obtained, it can indicate the corrosion started at a late stage, when the current density value started to rise. This can indicate possible initiations of a corrosion attack, but a longer test is needed to determine the actual behaviour later on.

The measured current values for sample 4 and 5 through the test are surprisingly low. Even though there are not any spalling of the coating, there are still brown spots at the coating surface that may indicate corrosion. This can be from water penetrating through small pores in the coating, but quickly plugged by corrosion products to stop further contact with water. The graphical data did not uncover any corrosion currents for these samples except for the first few hours. The corrosion probably occurred during these hours, and stopped due to the plugging of the pores initially present.



The values measured from the 45 degree spray samples are low compared to the samples with 90 degree spray angle. Even the maximum corrosion value measured on sample 6, are less than 10% of the values measured from Figure 44.

The polarized value was double checked with a multimeter though the test, to check if the real polarization value was -350mV vs. Ag/AgCl. The resistances used was also checked if the real resistance provided was actually 10 $\Omega$ . These parameters proved to be correct. There could still be defects in the wires used which cause wrong measurements. However, by comparing the samples to the data given in the graphical presentation, the measured results seem to be correct.

## 5.8 Erosion

The sand feed during the test did not achieve the 18wt% from the specification demand. With the current nozzle diameter, and a water velocity of 5 m/s, this high amount of sand in water would nearly consume well over 50 grams of sand each second. This means 180kg/h, which is not possible for a test of this scale.

The water supply was not constant throughout the test, and this had to be regulated manually, thus causing some uncertainty of the water velocity. However, as the deviation in flow rate were 1 l/min, this led to a difference in water velocity of about 0,23 m/s, which is 5%. In addition, these deviations did not last very long, as they were corrected in intervals of a few minutes.

The amount of sand in the water slurry was set to maximum feed. To keep the slurry velocity at 5m/s, the wt% of sand had to stay at this level. To get 18wt% sand in the water, the flow rate would have to be reduced to 0,78m/s. This would probably give a very low erosion effect, and a water velocity of 5m/s was therefore chosen instead.

The weight measurements showed no difference in weight before and after the test. According to the data sheet for the Amperit 560 coating (appendix 9.2), the density of the coating phases are 3,8-4,4 and 3,8-4,6 g/cm<sup>3</sup>. For a coating with a thickness of 0,35mm, 1g of coating corresponds to an area of about 7cm<sup>2</sup>. The size of the visible eroded area is about 5cm. This means a weight difference of 1g corresponds to the coating being completely eroded in an area larger than the exposed area. To use the weight measurement as a source of the erosion properties, the test should use a weight scale that measures the weight with more decimals. The test could also be done for a longer time to possibly erode the coating and reach the substrate. However, this would require a high amount of abrasive sand, and would be very time consuming considering the sand would need to be manually fed and removed from the test rig by a person.

The roughness values measured outside the exposed area shows less roughness compared to the values measured in the separate roughness test in the report. This may be because the roughness values from the erosion tests were measured after the test was done. Small amounts of the erosive slurry will splash around the impact area and cause some erosion on the rest of the test sample.

The roughness measurements of the samples showed a difference in the eroded area compared to the non-eroded area. This means the abrasive sand had some effect on the coating, but mainly on the roughness peaks.

The testing had to be aborted due to a breakdown of the motor supplying the abrasive sand. The sample thermally sprayed 90 degrees with an erosive jet angle of 60 degrees were thus not tested.

As the test rig were ready for testing close to the deadline for this project, there were not enough time to find a spare motor or do the cross section examination. A cross section examination of the samples to document any thickness reductions of the coating should be done as this were not done due to a lack of time.

## 6 Conclusion

The tests to document the main requirements for the coating were performed successfully.

Corrosion tests showed poor corrosion properties for samples sprayed 90 degrees, but better results for samples sprayed 45 degrees.

The erosion test showed good properties for all of the test samples. Not all of the results were analysed completely as the test rig were finished close to the end of the project. The time aspect affected the testing time of the samples as well. Testing of the samples for a longer period of time is advised to receive results of higher quality.

The mechanical properties of the coating showed promising results, but some adjustments should be done for future research. The bending test uncovered the expected results. The adhesion test did not experience the expected loads, but this was due to early rupture in the bonding agent and not in the coating itself. The impact test need adjustments proposed to give qualitative results. Hardness values measured were acceptable.

## 7 Future work

The corrosion properties of the coating needs to be improved to qualify for an approved solution. The thermal spray angle of 90 degrees are usually the optimal, but shows bad results compared to 45 degrees in the corrosion test.

The adhesion test did not document the adhesion strength of the coating due to weakness in the bonding agent. To do this test properly, a stronger bonding agent is needed. A test rig that can compensate for shear stresses in the samples would also be favourable as the shear stresses present may influence the results.

To qualify the coating roughness to the standard proposition, a surface treatment will need to be done.

The erosion test gave usable results, but as the motor supplying the abrasive sand broke down, the test were not finished. A sample thermally sprayed 90 degrees with an erosive jet of 60 degrees are not done in this report. A test using these parameters should be done to give a complete documentation of the erosion resistance for the parameters specified in the demand specification.

Impact test should be done on thicker and larger plates. The thin material thickness of the test plates affected the cracking of the coating. Even though these results are representable for pipes with thin walls, the actual coating behaviour under impact should be documented as well. By using thicker test plates, a reduced deformation is expected. This would provide information if the coating cracks due to deformation of the substrate or due to forces internally in the coating. Testing of the impact behaviour of the coating should be tested on the present material type and thickness of the pipes, as this gives information accurate to the real case.

## 8 References

- [1] Kravspesifikasjon, 2014.
- [2] F. Mubarok and N. Espallargas, Thermal spray coatings, slides, 2014.
- [3] S. Kuroda, J. Kawakita, M. Watanabe and H. Katanoda, Warm spraying—a novel coating process based on high-velocity impact of solid particles, 2008.
- [4] ASM International, Thermal spray technology, volume 5A, 2013.
- [5] “Cold spray coating process,” [Online]. Available: <http://www.gordonengland.co.uk/coldspray.htm>.
- [6] M. Couto, S. Dosta and J. M. Guilemany, Comparison of the mechanical and electrochemical properties of WC-17 and 12Co coatings onto Al7075-T6 obtained by high velocity oxy-fuel and, 2014.
- [7] NORSOK M-630, 2015.
- [8] ASTM C633, 2015.
- [9] ISO 6272-1, Rapid deformation (impact resistance) tests, 2011.
- [10] DNV C2, DNV electro chemical porosity test, 2015.
- [11] NTNU, Surfaces in contact, friction, lecture notes, 2014.
- [12] Mitutoyo, JIS B601:2001, geometric product specifications (gps) - surface texture: profile method, 2001.
- [13] S. Armada and S. Wilson, Test procedure: Korrosjon- og slitasjebeskyttelse av glatte metallflater WP3, 2014.
- [14] 3M, Scotch-weld epoxy adhesives 2214, technical data sheet, 1998.
- [15] J. Johansen, Erosion resistance of composite materials exposed to a mixture of water and sand, master thesis, 2014.
- [16] A. O. Bredesen, Internal thermal coating in pipe, 2014.
- [17] “Conversion Chart Abrasives - Grit Sizes,” [Online]. Available: <https://www.fine-tools.com/G10019.html>.
- [18] N. Espallargas, Thermal spray coatings, lecture notes, 2010.
- [19] NTNU, Wear, lecture notes, 2014.

[20] J. R. Laguna-Camacho, M. Vite-Torres, E. Gallardo-Hernández and E. Vera-Cárdenas, Solid Particle Erosion on Different Metallic Materials, 2013.

[21] “Designing with Metals: Dissimilar Metals and The Galvanic Series,” [Online]. Available: <http://www.ianosbackfill.com/specifications/>.

## 9 Appendix



## 9.1 Master thesis assignment text

NORGES TEKNIŠK-  
NATURVITENSKAPELIGE UNIVERSITET  
INSTITUTT FOR PRODUKTUTVIKLING  
OG MATERIALER

### **MASTEROPPGAVE VÅR 2015 FOR STUD.TECHN. ANDRÉ SUNDE**

**Egenskaper til termisk sprøytete belegg for bruk innvendig i rør og bend**

*Properties of thermal sprayed coatings for internal use in pipes and bends*

NTNU/SINTEF deltar i et forskningsprosjektet "Glatte flater" som finansieres av Norges Forskningsråd gjennom MAROFF programmet. Brunvoll, Triplex, Hustadmarmor og Aquamarine AS er industripartnere i prosjektet. En av aktivitetene i prosjektet (Aktivitet 3) har tittelen "Innvendig korrosjons- og slitasjebeskyttelse av rør ved hjelp av termisk sprøyting". I dag benyttes rustfrie rør med innvendig keramisk belegg som støpes inn i rørsegmenter. Dette er en kostbar løsning samtidig som vekten av rørsystemet er stor og det er ikke mulig å benytte standard rørdeler. Målsettingen med Aktivitet 3 i MAROFF prosjektet er å fremskaffe i) nødvendig sprøyteutstyr for å belegge min. 3 m rørlengder (inkludert bend) og ii) belegg som tilfredsstiller bestemte krav til korrosjons- og slitasjebestandighet i under aktuelle driftsbetingelser.

Aquamarine har anskaffet utstyr som er kan benyttes til innvendig belegning i rør. Utfordringen med innvendig belegning av rør inkludert bend er at viktige sprøyteparametere som bl.a. avstand til overflaten og sprøytevinkel ikke vil være konstant og optimal for å oppnå et belegg med best mulig egenskaper. Målsettingen med dette MSc prosjektet er å dokumentere de viktigste egenskapene til termisk sprøytet belegg utført med parametere som simulerer innvendig sprøyting. Egenskapene som skal dokumenteres er; slitasje, korrosjon, hardhet, duktilitet og porøsitet. I tillegg skal belegget karakteriseres i SEM. Det er utarbeidet en egen testprotokoll for gjennomføring av testene.

I tillegg til å utføre testing av ulike belegg, skal MSc studenten sette seg inn i ulike metoder for termisk sprøyting og ulike typer belegg for ulike anvendelser. Studenten skal også sette seg inn i bakgrunnen for, gjennomføringen av og tolkningen av resultatene fra de ulike testene som gjennomføres.

Prosjektarbeidet vil gjennomføres i nær kontakt med representanter for industribedriftene og SINTEF.

#### **Formelle krav:**

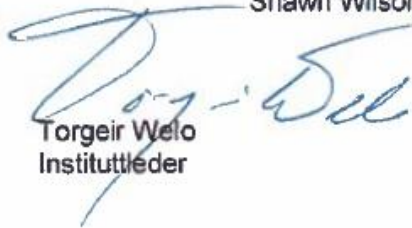
Senest 3 uker etter oppgavestart skal et A3 ark som illustrerer arbeidet leveres inn. En mal for dette arket finnes på instituttets hjemmeside under menyen masteroppgave (<http://www.ntnu.no/ipm/masteroppgave>). Arket skal også oppdateres en uke før innlevering av masteroppgaven.

Risikovurdering av forsøksvirksomhet skal alltid gjennomføres. Eksperimentelt arbeid definert i problemstilling skal planlegges og risikovurderes innen 3 uker etter utlevering av oppgavetekst. Konkrete forsøksvirksomhet som ikke omfattes av generell risikovurdering skal spesielt vurderes før eksperimentelt arbeid utføres. Risikovurderinger skal signeres av veileder og kopier skal inngå som vedlegg til oppgaven.

Besvarelsen skal ha med signert oppgavetekst, og redigeres mest mulig som en forskningsrapport med et sammendrag på norsk og engelsk, konklusjon, litteraturliste, innholdsfortegnelse, etc. Ved utarbeidelse av teksten skal kandidaten legge vekt på å gjøre teksten oversiktlig og velskrevet. Med henblikk på lesning av besvarelsen er det viktig at de nødvendige henvisninger for korresponderende steder i tekst, tabeller og figurer anføres på begge steder. Ved bedømmelse legges det stor vekt på at resultater er grundig bearbeidet, at de oppstilles tabellarisk og/eller grafisk på en oversiktlig måte og diskuteres utførlig.

Besvarelsen skal leveres i elektronisk format via DAIM, NTNUs system for Digital arkivering og innlevering av masteroppgaver.

Kontaktperson: Roy Liltvedt, Aquamarine  
Shawn Wilson, SINTEF



Torgeir Welo  
Instituttleder



Roy Johnsen  
Faglærer



NTNU  
Norges teknisk-  
naturvitenskapelige universitet  
Institutt for produktutvikling  
og materialer

## 9.2 Datasheet for WC-Co (83/17) / NiSF RC 60 50-50



POWDERS FOR THERMAL SPRAYING

Number  
Issue

PD-4034  
5-17.12.2013

### AMPERIT® 560

<b>Chemical Formula</b>	WC-Co(83-17) / NISF RC 60 50-50
<b>Chemical Name</b>	Tungsten Carbide-Cobalt(83-17)-Nickel-SF RC 60 50-50
<b>Description of Product</b>	Blended
<b>Grades Available</b>	<b>Product Designation</b>
	AMPERIT® 560.062 53/10 µm
	AMPERIT® 560.077 63/32 µm

#### Chemical Characteristics

(Mass fraction in % [cg/g]; ppm [µg/g])

	WC-Co 83-17		Ni-SF RC 60
Co	15.0 - 18.0 %	Cr	14.2 - 16.5 %
Fe	max. 0.2 %	Fe	3.5 - 4.5 %
C <sub>tot</sub>	4.9 - 5.3 %	Si	4.0 - 4.8 %
W	balance	B	3.0 - 3.9 %
		C	0.6 - 1.0 %
		Ni	balance

#### Physical Characteristics

Particle Size Distribution	WC-Co 83-17 for 63/32 µm	Ni-SF RC 60 for both grain sizes
+ 63 µm	max. 5 % <sup>2)</sup>	max. 2 % <sup>3)</sup>
+ 53 µm		max. 10 % <sup>3)</sup>
- 38 µm	max. 20 % <sup>2)</sup>	
- 32 µm		max. 12 % <sup>3)</sup>
Apparent Density acc. ASTM B 212	3.8 - 4.4 g/cm <sup>3</sup>	3.8 - 4.6 g/cm <sup>3</sup>

Particle Size Distribution	WC-Co 83-17 for 53/10 µm
- 88 µm	max. 100 % <sup>1)</sup>
D 90 %	51 - 59 µm
D 50 %	31 - 37 µm
D 10 %	17 - 22 µm
Apparent Density acc. ASTM B 212	3.8 - 4.4 g/cm <sup>3</sup>

1) MICROTRAC by Laser Light Diffraction per ASTM C 1070, 2) ROTAP Screening per ASTM B 214,  
3) ALPINE Air Jet Screening.

### 9.3 Hardness measurements

The measurement sections is illustrated in Figure 58.

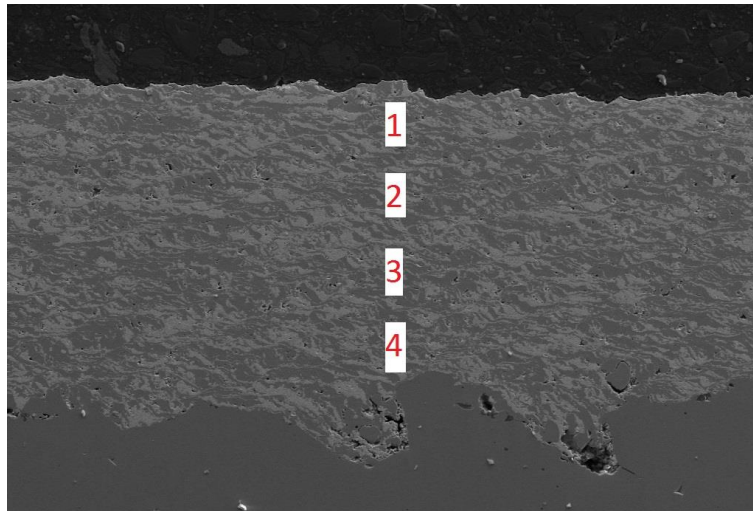


Figure 58: The four sections of hardness measurement in the coating

Table 21: Hardness measurements for 45 degree spray angle

45 degree spray angle								
Section	Hardness value (HV)							
1	664	811	747	646	701	754	788	676
2	810	881	824	789	821	815	754	803
3	841	817	813	843	825	832	840	789
4	848	835	736	873	829	838	815	692

Table 22: Hardness measurements for 90 degree spray angle

90 degree spray angle				
Section	Hardness value (HV)			
1	579	970	991	712
2	791	639	962	761
3	898	1179	748	852
4	792	951	905	695

## 9.4 Bending test pictures

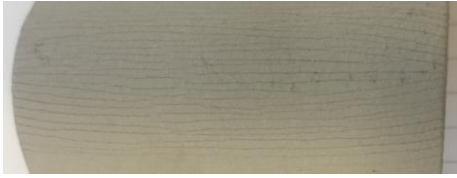


**Figure 59: Bending test sample 2**

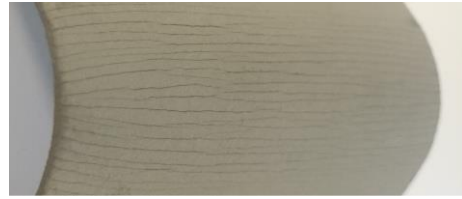


**Figure 60: Bending test sample 3**



**Figure 61: Bending test sample 4**



**Figure 62: Bending test sample 5**



**Figure 63: Bending test sample 6**



**Figure 64: Bending test sample 7**



**Figure 65: Bending test sample 8**

## 9.5 Adhesion test rupture locations



Figure 66: Adhesion test sample 3

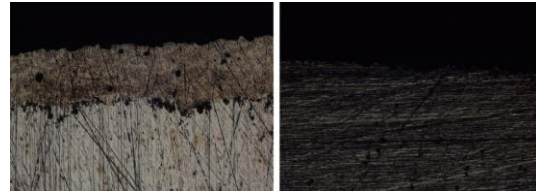


Figure 67: Adhesion test sample 4

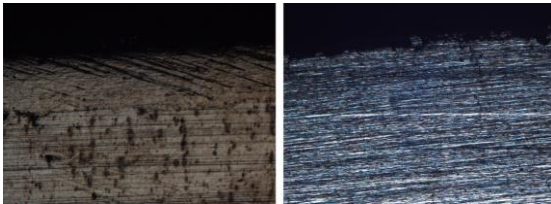


Figure 68: Adhesion test sample 5

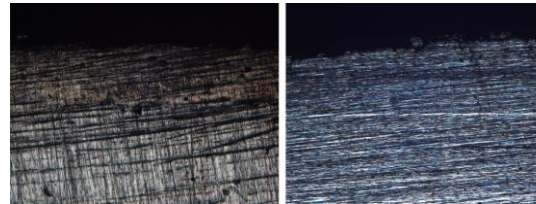


Figure 69: Adhesion test sample 6

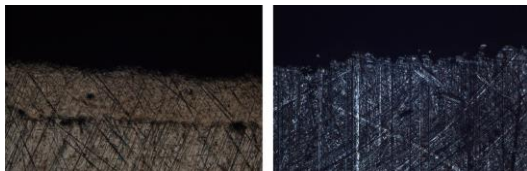


Figure 70: Adhesion test sample 7

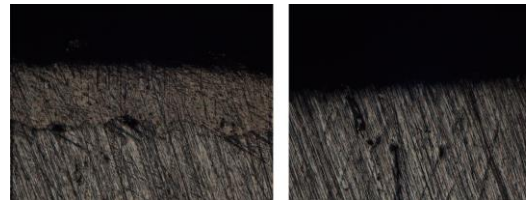


Figure 71: Adhesion test sample 8



Figure 72: Adhesion test sample 9

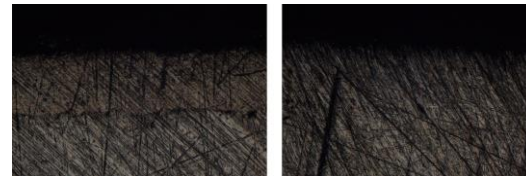


Figure 73: Adhesion test sample 10

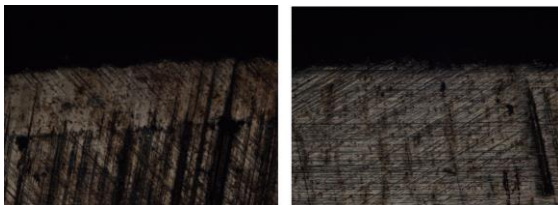


Figure 74: Adhesion test sample 11

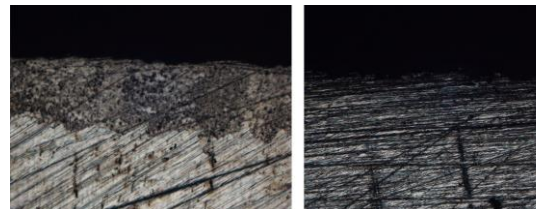



Figure 75: Adhesion test sample 12

## 9.6 Risk assessment part 1

**Detaljert Risikoreport (ny)**

---

<b>ID</b>	203	<b>Status</b>	<b>Dato</b>
<b>Risikoområde</b>	Risikovurdering: Helse, miljø og sikkerhet (HMS)	Opprettet	17.02.2015
<b>Opprettet av</b>	André Sunde	Vurdering startet	24.02.2015
<b>Ansvarelig</b>	Nousha Kheradmand	Tiltak besluttet	
		Avsluttet	

### Metallography lab for André Sunde

**Gyldig i perioden:**  
2/17/2015 - 6/17/2018

**Mål / hensikt**  
Risk assesment on the activity in the metallurgy lab

**Bakgrunn**  
The assessment are made to ensure safe working conditions and avoid accident

**Beskrivelse og avgrensninger**  
1. Cutting samples  
2. Microscopy analysis  
3. Hardness test

**Forutsetninger, antakelser og forenklinger**  
Every new activity on the metallurgy lab should be assessed and registered in addition to the existing one

**Vedlegg**  
[Ingen registreringer]

**Referanser**  
[Ingen registreringer]

---

<b>Norges teknisk-naturvitenskapelige universitet (NTNU)</b> Unntatt offentlighet jf. Offentlighetsloven § 14	<b>Utskriftsdato:</b> 04.03.2015	<b>Utskrift foretatt av:</b> André Sunde	<b>Side:</b> 1/9
--	-------------------------------------	---	---------------------



### Oppsummering, resultat og endelig vurdering

I oppsummeringen presenteres en oversikt over farer og uønskede hendelser, samt resultat for det enkelte konsekvensområdet.

**Forekilde:** Cutting activity

**Uønsket hendelse:** Broken cutting machine

**Konsekvensområde:** Ytre miljø

Risiko før tiltak:  Risiko etter tiltak:

Materielle verdier

Risiko før tiltak:  Risiko etter tiltak:

**Uønsket hendelse:** Flying debris

**Konsekvensområde:** Helse

Risiko før tiltak:  Risiko etter tiltak:

**Forekilde:** Microscopy analysis

**Uønsket hendelse:** Scratching the optic of microscope

**Konsekvensområde:** Materielle verdier

Risiko før tiltak:  Risiko etter tiltak:

**Uønsket hendelse:** Hot lamp area

**Konsekvensområde:** Helse

Risiko før tiltak:  Risiko etter tiltak:

Materielle verdier

Risiko før tiltak:  Risiko etter tiltak:

**Forekilde:** Vickers hardness measurement

**Uønsket hendelse:** Broken equipment

**Konsekvensområde:** Materielle verdier

Risiko før tiltak:  Risiko etter tiltak:

### Endelig vurdering





### Oversikt involverte enheter og personell

En risikovurdering kan gjelde for en, eller flere enheter i organisasjonen. Denne oversikten presenterer involverte enheter og personell for gjeldende risikovurdering.

#### Enhet /-er risikovurderingen omfatter

- Norges teknisk-naturvitenskapelige universitet

#### Deltakere

[Ingen registreringer]

#### Lesere

Roy Johnsen  
Afrooz Barnoush

#### Andre involverte/interessenter

[Ingen registreringer]

Følgende akseptkriterier er besluttet for risikoområdet Risikovurdering: Helse, miljø og sikkerhet (HMS):

#### Helse



#### Materielle verdier



#### Omdømme



#### Ytre miljø



**Oversikt over eksisterende, relevante tiltak som er hensyntatt i risikovurderingen**

I tabellen under presenteres eksisterende tiltak som er hensyntatt ved vurdering av sannsynlighet og konsekvens for aktuelle uønskede hendelser.

Farekilde	Ønsket hendelse	Tiltak hensyntatt ved vurdering
Cutting activity	Broken cutting machine	Training for equipment
	Flying debris	Training for equipment
Microscopy analysis	Scratching the optic of microscope	Training for equipment
	Hot lamp area	Training for equipment
Vickers hardness measurement	Broken equipment	Training for equipment

**Eksisterende og relevante tiltak med beskrivelse:****Training for equipment**

Individual training are given on each equipment in the laboratory based on the need

**Training of using the room**

All participants that work in the labs are informed about the importance of using protective equipment, first-aid kits, emergency exit, emergency shower, fire-fighting and waste management

**Trainor HSE e-course**

It is obligatory to follow HSE e-training courses provided by trainor

**Access control**

Only those who follow all the necessary training are given access to the laboratory.

**Risikoanalyse med vurdering av sannsynlighet og konsekvens**

I denne delen av rapporten presenteres detaljer dokumentasjon av de farer, uønskede hendelser og årsaker som er vurdert. Innledningsvis oppsummeres farer med tilhørende uønskede hendelser som er tatt med i vurderingen.

**Følgende farer og uønskede hendelser er vurdert i denne risikovurderingen:**

- **Cutting activity**
  - Broken cutting machine
  - Flying debris
- **Microscopy analysis**
  - Scratching the optic of microscope
  - Hot lamp area
- **Vickers hardness measurement**
  - Broken equipment

**Oversikt over besluttede risikoreduerende tiltak med beskrivelse:**



### Cutting activity (farekilde)

Broken cutting machine

#### Cutting activity/Broken cutting machine (uønsket hendelse)

The incorrect setting of the machine may lead to broken cutting wheel, damping or clogging the machine, damaging the sample stage and motor and damaging/destroying the samples.

#### Identifiserte årsaker til hendelsen

Samlet sannsynlighet vurdert for hendelsen: Lite sannsynlig (2)

Kommentar til vurdering av sannsynlighet:

Operator should have specific training for the tool

#### Vurdering av risiko for følgende konsekvensområde: Ytre miljø

Vurdert sannsynlighet (felles for hendelsen): Lite sannsynlig (2)

Vurdert konsekvens: Liten (1)

Kommentar til vurdering av konsekvens:

[Ingen registreringer]



#### Cutting activity/Flying debris (uønsket hendelse)

The debris from cutting activity would fly and hurt user if the lid/door are opened before the wheel stops completely

#### Identifiserte årsaker til hendelsen

Samlet sannsynlighet vurdert for hendelsen: Lite sannsynlig (2)

Kommentar til vurdering av sannsynlighet:

- 1) The lid stops debris from coming out. It is not possible to open it while the cutting occurs.
- 2) Operator uses goggles.

#### Vurdering av risiko for følgende konsekvensområde: Helse

Vurdert sannsynlighet (felles for hendelsen): Lite sannsynlig (2)

Vurdert konsekvens: Liten (1)

Kommentar til vurdering av konsekvens:

[Ingen registreringer]





**Microscopy analysis (farakilde)**

**Microscopy analysis/Scratching the optic of microscope (uønsket hendelse)**

**Identifiserte årsaker til hendelsen**

*Optic gets scratched from contact with sample*

Magnifying the sample without being aware of the position of the optic, may cause the sample to come in contact with the optic and cause damage

Samlet sannsynlighet vurdert for hendelsen: Lite sannsynlig (2)

Kommentar til vurdering av sannsynlighet:

[Ingen registreringer]

**Vurdering av risiko for følgende konsekvensområde: Materielle verdier**

Vurdert sannsynlighet (felles for hendelsen): Lite sannsynlig (2)

Vurdert konsekvens: Stor (3)

Kommentar til vurdering av konsekvens:

[Ingen registreringer]



**Microscopy analysis/Hot lamp area (uønsket hendelse)**

**Identifiserte årsaker til hendelsen**

*Not turned off*

The lamp is not turned off after use

Samlet sannsynlighet vurdert for hendelsen: Sannsynlig (3)

Kommentar til vurdering av sannsynlighet:

[Ingen registreringer]

**Vurdering av risiko for følgende konsekvensområde: Helse**

Vurdert sannsynlighet (felles for hendelsen): Sannsynlig (3)

Vurdert konsekvens: Liten (1)

Kommentar til vurdering av konsekvens:

[Ingen registreringer]





### Vickers hardness measurement (farekilde)

#### Vickers hardness measurement/Broken equipment (uønsket hendelse)

Working with vickers microhardness should be done really carefully as this machine is very sensitive to movement

#### Identifiserte årsaker til hendelsen

*Improper use of equipment*

Samlet sannsynlighet vurdert for hendelsen: Lite sannsynlig (2)

Kommentar til vurdering av sannsynlighet:

[Ingen registreringer]

#### Vurdering av risiko for følgende konsekvensområde: Materielle verdier

Vurdert sannsynlighet (felles for hendelsen): Lite sannsynlig (2)

Vurdert konsekvens: Stor (3)

Kommentar til vurdering av konsekvens:

[Ingen registreringer]





**Oversikt over besluttede risikoreducerende tiltak:**

Under presenteres en oversikt over risikoreducerende tiltak som skal bidra til å redusere sannsynlighet og/eller konsekvens for uønskede hendelser.

**Oversikt over besluttede risikoreducerende tiltak med beskrivelse:**



*Per Lø*

*André Sunde*

*A. K. Sunde*

9.7 Risk assessment part 2

NTNU	Kartlegging av risikofylt aktivitet			Utdragsdel av	Nummer	Dato
				FMS-ved. Godkjent av	FMSRY2601	22.03.2011
FMS				Praktis		Erstatte 01.12.2006

Enhet: **IPM**

Dato: **27.01.2015**

Linjeleder: **Roy Johnsen**

Delegerere ved kartleggingen (mv funksjon): **André Sunde, Student**

(Ansv. veileder, student, evt. medveiledere, evt. andre m. kompetanse)

**Kort beskrivelse av hovedaktivitet/hovedprosess:** Testing av mekaniske og kjemiske egenskaper til coating i korrosjonslab

**Er oppgaven rent teoretisk? (JA/NEI):** **Nei** "Ja" betyr at veileder inneslår for at oppgaven ikke inneholder noen aktiviteter som krever risikovurdering. Dersom "Ja": Beskriv kort aktiviteten i kartleggingskjemnet under. Risikovurdering henger ikke å fylles ut.

**Signaturer:** Ansvartlig veileder: 

Student: 

ID nr.	Aktivitet/prosess	Ansvartlig	Ekisterende dokumentasjon	Ekisterende sikringsstiltak	Lov, forskrift o.l.	Kommentar
1	Elektrokjemisk porositetstest	André	Interne prosedyrer for labarbeid på NTNU	Vernestyr, Godkjent utstyr		
2	Erosjonstest	André	Interne prosedyrer for labarbeid på NTNU	Vernestyr, Godkjent utstyr		
3	Sløttest	André	Interne prosedyrer for labarbeid på NTNU	Vernestyr, Godkjent utstyr		
4	Adhesjonstest	André	Interne prosedyrer for labarbeid på NTNU	Vernestyr, Godkjent utstyr		
5	Boyetest	André	Interne prosedyrer for labarbeid på NTNU	Vernestyr, Godkjent utstyr		
6	Rutetelling	André	Interne prosedyrer for labarbeid på NTNU	Vernestyr, Godkjent utstyr		



NTNU	Utbetjning av	Nummer	Dato
HMS	HMS-avd.	HMSRIV2601	22.03.2011
	Godkjent av		Erstatter
	Punkt		01.12.2006

## Risikovurdering

Dato: 27.01.2015

Ehnet: IPM  
Linjeleder: Roy Johnsen

Deltaere ved kartleggingen (mv funksjon): André Sunde, Student

(Ansv. Veileder, student, evi, medveileder, ev. andre m. kompetanse)

Risikovurderingen gjelder hovedaktivitet: Testing av mekaniske og kjemiske egenskaper til coating

Signaturer: Ansvartlig veileder: *Roy Johnsen* Student: *André Sunde*

ID nr	Aktivitet fra kartleggings-skjemaet	Mulig uønsket hendelse/ belastning	Vurdering av sannsynlighet (1-5)	Vurdering av konsekvens:			Risiko-Verdi (menn-esse)	Risiko-verdi (andre parametre)	Kommentarer/status Forslag til tiltak
				Menneske (A-E)	Ytre miljø (A-E)	ØK/ material (A-E)			
1a	Elektrokjemisk porositest	Elektrode kørner under forsøk	3	A	A	A	A3	Sikre at all utstyr sitter godt fast og passe på at det ikke ligger utsatt til for at andre kommer bort utstyr under forsøket.	
1b	Elektrokjemisk porositest	Glasskåbe faller i bakken og knuser	3	A	A	A	A3	Passer på at testen ikke ligger utsatt til for å falle.	
1c	Elektrokjemisk porositest	Aceton på hud eller i øyne under rensing av prøver	3					Aceton gir ikke skade som krever førstehjelp, som er et krav til å være konsekvens "A". Det kan likevel gi irritasjon på hud og øyne ved kontakt og det bør derfor brukes verneutstyr.	
2a	Erosjonstest	Vannlåsje	2		B		B2	Sjekk koblinger før bruk. Skru av etter bruk.	

NTNU		Utskriftet av	Nnummer	Dato
		HMS-avd.	HMSRV2501	22.03.2011
HMS		Godkjent av		Erstatner
		Følefor		01.12.2006
<b>Risikovurdering</b>				

2b	Erosjonstest	Personskade fra vann under trykk	2	B		B2		Sikre koblinger. Skru av etter bruk
2c	Erosjonstest	Støvforurensing av luft	3	C	A	C3	A3	Ventilasjon av rom. Bruke eksisterende deksel. Maske
2d	Erosjonstest	Tette sluk med sand	4		B	B	B4	Bruke skillevegg i tank. Tørnne tank etter endt test.
3a	Slagtest	Fingre i klem mellom kule og prøve	3	B		B	B3	Sikre fallende kule før test. Feste prøven før kulen settes opp.
3b	Slagtest	Bitler slås løs under testling og treller øve	2	B		B	B2	Bruke vernebriller. Hold avstand fra testen.
4a	Adhesjonstest	Skade på utstyr	2		B		B2	Utføre arbeid etter instruks
5a	Boyetest	Skade på utstyr	2		C		C2	Utføre arbeid korrekt
5b	Bøyetest	Komne i klem under bøyning	2	B		C	B2	Være obs når det bøyes. Ikke røre utstyr under forsøk
6a	Ruhestmåling	Skade på utstyr	2		B		B2	Utføre arbeid etter instruks

**Sannsynlighet vurderes etter følgende kriterier:**

Svært liten 1	Liten 2	Middels 3	Stor 4	Svært stor 5
1 gang pr 50 år eller sjeldnere	1 gang pr 10 år eller sjeldnere	1 gang pr år eller sjeldnere	1 gang pr måned eller sjeldnere	Stjer ukentlig

**Konsekvens vurderes etter følgende kriterier:**

Gradering	Mannskape	Vite miljø	Økt/materiell	Ordmenn
E Svært alvorlig	Død	Vann, jord og luft Svært langvarig og ikke reversibel skade	Drifts- eller aktivitetstans > 1 år.	Troverdighet og respekt betydelig og varig svekket
D	Alvorlig personskade.	Langvarig skade. Lang	Driftstans > 1/2 år	Troverdighet og respekt

NTNU		Utarbeidet av	Nummer	Dato	
		HMS-avd.	HMSRUV2801	22.03.2011	
HMS		Godkjent av		Etabler	
		Risikør		01.12.2006	
<b>Risikovurdering</b>					

<b>Alvorlig</b>	Maling utenfrel.	restitusjonstid	Aktivitetstans i opp til 1 år	betydelig svekket
<b>C Moderat</b>	Alvorlig personskade.	Mindre skade og lang restitusjonstid	Drille- eller aktivitetstans < 1 mnd	Troværdighet og respekt svekket
<b>B Liten</b>	Skade som krever medisinsk behandling	Mindre skade og kort restitusjonstid	Drills- eller aktivitetstans < 1 uke	Negativ påvirkning på troværdighet og respekt
<b>A Svært liten</b>	Skade som krever førstehjelp	Ubetydelig skade og kort restitusjonstid	Drills- eller aktivitetstans < 1 dag	Liten påvirkning på troværdighet og respekt

**Risikoverdi = Sannsynlighet x Konsekvens**

Beregn risikoverdi for Menneske. Enheten vurderer selv om de i tillegg vil beregne risikoverdi for Ytre miljø, Økonomi/materiell og Omdømme. I så fall beregnes disse hver for seg.

**Til kolonnen "Kommentarer/status, forslag til forebyggende og korrigerende tiltak":**

Tiltak kan påvirke både sannsynlighet og konsekvens. Prioriter tiltak som kan forhindre at hendelsen inntreffer, dvs. sannsynlighetsreducerende tiltak foran skjerpet beredskap, dvs. konsekvensreducerende tiltak.

NTNU		Utdelt av		Nummer		Dato	
		HMS-ansv.		HMS/RV2004		08.03.2010	
HMS/MS		godkjent av		Ersatter			
		Faktor		09.02.2010			

**Risikomatrix**

**MATRISE FOR RISIKOVURDERINGER ved NTNU**

		<b>KONSEKVENNS</b>					
Svært alvorlig	<b>E1</b>	<b>E2</b>	<b>E3</b>	<b>E4</b>	<b>E5</b>		
Alvorlig	<b>D1</b>	<b>D2</b>	<b>D3</b>	<b>D4</b>	<b>D5</b>		
Moderat	<b>C1</b>	<b>C2</b>	<b>C3</b>	<b>C4</b>	<b>C5</b>		
Liten	<b>B1</b>	<b>B2</b>	<b>B3</b>	<b>B4</b>	<b>B5</b>		
Svært liten	<b>A1</b>	<b>A2</b>	<b>A3</b>	<b>A4</b>	<b>A5</b>		
	Svært liten	Liten	Middels	Stor	Svært stor		
	<b>SANNSYNLIGHET</b>						

Prinsipp over akseptkriterium. Forklaring av fargene som er brukt i risikomatrixen.

Farge	Beskrivelse
Rødt	Uakseptabel risiko. Tiltak skal gjennomføres for å redusere risikoen.
Gul	Vurderingsområde. Tiltak skal vurderes.
Grøn	Akseptabel risiko. Tiltak kan vurderes ut fra andre hensyn.